ELSEVIER

Contents lists available at ScienceDirect

Forest Ecology and Management

journal homepage: www.elsevier.com/locate/foreco





Fire after clear-cut harvesting minimally affects the recovery of ecosystem carbon pools and fluxes in a Great Lakes forest

Cameron Clay ^{a,*}, Luke Nave ^b, Knute Nadelhoffer ^c, Christoph Vogel ^b, Brooke Propson ^d, John Den Uyl ^b, Laura J. Hickey ^a, Alexandra Barry ^e, Christopher M. Gough ^a

- ^a Department of Biology, Virginia Commonwealth University, Richmond, VA, USA
- ^b Biological Station and Department of Ecology and Evolutionary Biology, University of Michigan, Ann Arbor, MI, USA
- Department of Ecology and Evolutionary Biology, University of Michigan, Ann Arbor, MI, USA
- ^d Department of Soil Science, University of Wisconsin-Madison, Madison, WI, USA
- e School of Forest Resources, University of Maine, Orono, ME, USA

ARTICLE INFO

Keywords:
Fire
Clearcut
Carbon
Succession
Compounding disturbance
Forests

ABSTRACT

Effective forest carbon (C) management requires an understanding of how stand-replacing disturbances affect C pools and fluxes over successional timescales, and how the growth of secondary forests compares with that of undisturbed forests. In the upper Great Lakes region, fires that followed clear-cut harvesting shaped a century-old cohort of secondary forests, but the long-term effects of fire on C cycling in this relatively fire-averse landscape remain poorly understood. We examined how two different stand-replacing disturbances - one with and the other without fire - influenced C pools and fluxes through a century of stand development, comparing secondary aspen-dominated (Populus) forests with legacy late successional stands encompassing the ages and species compositions that would be prevalent today in the absence of stand replacement. Our work at the University of Michigan Biological Station (UMBS) used experimental forest chronosequences established following clear-cut harvesting or clear-cut harvesting followed by fire, along with three > 130-yr-old late successional deciduous broadleaf (DBF), evergreen needleleaf (ENF), and mixed (MIX) forest functional types. The successional trajectories and values of total (above- and belowground) ecosystem C mass, net primary production (NPP), and net ecosystem production (NEP) were similar regardless of whether fires occurred following clear-cut harvesting. Moreover, 80 + year old secondary forests' C pools and fluxes were comparable to late successional ENF and MIX, but were at times lower than DBF. While the century-old secondary forests and legacy stands served as consistent C sinks over the last century, more extreme temperatures in recent years may be eroding NEP by accelerating C losses from soils. We conclude that the compounding effects of fire and clear-cut harvesting were similar to those from clear-cut harvesting alone, possibly because of the disturbance-adapted properties of pioneer species, most notably aspen; however, our results also suggest that changing climate rather than prior disturbance may jeopardize the future of this long-term terrestrial C sink.

1. Introduction

North America's secondary temperate forests have been a stable terrestrial carbon (C) sink for over a century (Birdsey et al. 2006), but the interacting effects of disturbance history and successional dynamics may affect the long-term trajectory of this critical ecosystem service (Pan et al. 2013, Williams et al. 2021). Most *Populus*-dominated maturing secondary forests of the upper Great Lakes region were established after early 20th century clear-cut harvesting that was often

followed by detritus-fueled fires (Kilburn 1960). This era of stand-replacing disturbances reset succession, abruptly changing the composition and structure of the region's late successional forests and depleting large reservoirs of C stored in biomass and soils (Curtis and Gough 2018). Now, as many unmanaged forests in the region approach a century of regrowth, the degree to which C pools and fluxes have recovered remains unclear. This lack of understanding stems from challenges associated with studying century-long C cycling processes, and a general deficiency of observations from late successional reference

^{*} Corresponding author at: 1000 W. Cary St., Richmond, VA 23284. E-mail address: cameronnss@gmail.com (C. Clay).

forests (Lorimer and Halpin 2014). Yet, such knowledge is fundamental to understanding the timing and extent of forest C recovery following stand-replacing disturbance (Amiro et al. 2010), honing predictions of future C cycling (Ma et al 2019), and managing and maintaining the terrestrial C sink (Birdsey et al. 2006).

Long-term temporal dynamics (i.e., succession trajectories) of forest C pools and fluxes depend on several factors, including the type and frequency of stand-replacing disturbance and the disturbance-adaptive strategies of impacted species. For example, the type or origin of disturbance influences the availability of growth-limiting factors, including nutrient capital, seedlings and seeds, and soil organic matter (Nave et al. 2010, Janssens et al. 2010, Cai et al. 2018). Specifically, clear-cut harvesting inherently reduces the number of seed trees supporting natural regeneration, and has been shown to suppress long-term soil nutrient recovery (Hendrickson et al. 2011). When detritus-fueled fire occurs after clear-cut harvesting, additional nutrients may be lost through leaching or volatilization (Certini 2005), and the seed bank size and seedling density may decline even more (Seidl et al. 2016, Cai et al. 2018). Consequently, relative to clear-cut harvesting only, the addition of fire could further lower the trajectory of ecosystem-wide C pool and flux recovery. Alternatively, fire-adapted species may display greater reproduction and growth following fire, supporting the rapid stand-level recovery of C pools and fluxes. For example, aspen populations, once established, reproduce clonally after severe fire and their fast-growing, shade intolerance may support relatively rapid and complete standscale recovery (Smith et al. 2011). However, while fire-C cycling studies are numerous (Thom and Seidl 2016), few provide comprehensive accounting of major C pools and fluxes over successional timescales in relation to legacy stands that avoided stand-replacing disturbance, which provide a critical benchmark for assessing the extent of recovery (sensu Hillebrand et al. 2018). Such C accounting is particularly rare for forests that, under natural fire regimes, experience long fire-return intervals (Malamud et al. 2005), such as much of the upper Great Lakes forested landscape (Whitney 1987).

With the goal of understanding how historical disturbances in the Great Lakes region affect contemporary C cycling, we documented century-long trends in the recovery of major forest C pools and fluxes, including total above- and belowground C stocks, bulk and heterotrophic soil respiration (R_s, R_{sh}), net primary production (NPP), and net ecosystem production (NEP) following clear-cut harvesting with and without fire. We utilized two experimental forest chronosequences, one cut-only and the other cut-and-burned at stand establishment, and compared C pools and fluxes in these secondary forests with three late successional plant functional types representing forest legacies that would be prominent on the landscape today in the absence of the large scale, historical stand-replacing disturbances of the early 20th century (Scheuermann et al. 2018, Wales et al. 2020). Our objectives were to: 1) identify whether successional changes in C pools and fluxes differ as a function of clear-cut harvesting with or without subsequent fire; and 2) quantify and compare the primary C pools and fluxes of secondary and legacy late successional forests. A related, secondary objective was to provide comparative C pool and flux data for late successional forests, providing important baseline and reference data for understudied century-old forests in the region (Tang et al. 2008, Tang et al. 2009). Because fire at our site may reduce soil nitrogen (N) availability over the long-term (White et al. 2004, Nave et al. 2019), and N availability is tightly coupled with plant growth and belowground C cycling processes at our site (Nave et al. 2009), we hypothesized that: 1) fire would further lower the successional trajectory (i.e., decrease the slope over time, sensu Ueyema et al. 2019) of C pools and fluxes, including total ecosystem C mass, NPP, NEP, and R_{sh}; and 2) as a result, forests established following clear-cut harvesting without fire would recover C pools and fluxes more rapidly and more closely approach levels observed in late successional forests.

2. Methods

2.1. Study site

Our study location is the University of Michigan Biological Station (UMBS), a ~ 4,000 ha mostly forested landscape near Pellston, Michigan (MI), in the northern Lower Peninsula (Fig. 1). The forests of this region experienced near universal stand-replacing clear-cut and fire initiated by European and Anglo-American settlers from the late 1800 s to the early 1900 s, with most severe large-scale forest disturbances terminating in the region in 1911. Forest composition varies depending on disturbance history, time since disturbance, and, in the case of latesuccessional stands, landform and soils (Lapin and Barnes 1995). Sitewide, dominant tree species include bigtooth aspen (Populus grandidentata), paper birch (Betula papyrifera), white pine (Pinus strobus), red pine (Pinus resinosa), American beech (Fagus grandifolia), red maple (Acer rubrum), northern red oak (Quercus rubra), trembling aspen (Populus tremuloides), balsam fir (Abies balsamea) and sugar maple (Acer saccharum). Soils at our study sites are generally excessively welldrained, coarse-textured Spodosols (>90% sand). The mean annual temperature is 5.5 °C and the mean annual precipitation is 817 mm. The growing season (i.e from green-up to leaf-off) typically spans late May through early October (Curtis et al. 2005).

Our study sites encompass 11 forest stands that are representative, but not fully comprehensive, of the region's diverse forest types, ages, and disturbance histories (Nave et al. 2017, Table 1): two forest chronosequences initiated following either clear-cutting (hereafter the "Cut Only" chronosequence) or clearcutting and fire (hereafter the "Cut and Burn" chronosequence), and three late successional stands representative of vegetation communities and structures that would presently occupy the region in the absence of stand-replacing disturbance. The "Cut Only" chronosequence consists of four, 0.4 to 1 ha stands that were clear cut in 1911, 1952, 1972, or 1987. The "Cut and Burn" chronosequence consists of four ~ 1 ha stands that were experimentally clear-cut harvested and burned in 1936, 1954, 1980, or 1998 (Gough et al. 2007). Prior to experimental clear-cutting and/or fire, chronosequence stand were mainly secondary aspen-dominated communities at various stages of recovery following region-wide disturbance in the early 20th century. Within each of these 11 stands, C pool and flux measurements were conducted in 2 to 3 circular or rectangular 0.1 ha plots, with total sampling plots number 29 study-wide. In the 1998 stand, one rectangular 0.06 ha plot and one rectangular 0.14 ha plot were sampled because other manipulations prevented circular plot arrangements. The three late successional legacy (hereafter "LS") stands include: 1) a red pine dominated stand (hereafter "ENF", for Evergreen Needle-Leaf) established c. 1890; 2) a deciduous broadleaf dominated stand ("DBF" for Deciduous Broadleaf) established c. 1833; and 3) a mixed coniferdeciduous forest ("MIX") established c. 1891. Since experiment initiation in 2014, American beech, a previously dominant canopy species, has dramatically declined in the DBF stand (Atkins et al. 2020) due to the spread of beech bark disease. We consider LS stands useful references, particularly given the paucity of observations for century-old forests in the region (Gough et al. 2016), but not precursors or endmembers of chronosequence stands, noting differences in soils and landform among LS and chronosequence stands (Nave et al. 2018).

2.2. Wood mass and net primary production

We estimated above- and belowground wood mass (M_{aw} , M_{bw}) and above- and belowground wood NPP (NPP_{aw}, NPP_{bw}) from repeated measurements of stem diameter and used allometric equations relating wood mass to diameter (Gough et al. 2007). Censuses of all trees larger than 8 cm diameter at breast height (dbh) were conducted in 2014 and 2019 in each plot. Biomass was estimated for live trees in 2014 and 2019 using species-specific allometries generated on site or in Midwestern and Eastern United States forests (Wiant 1977, Ker 1980, Young et al. 1980,

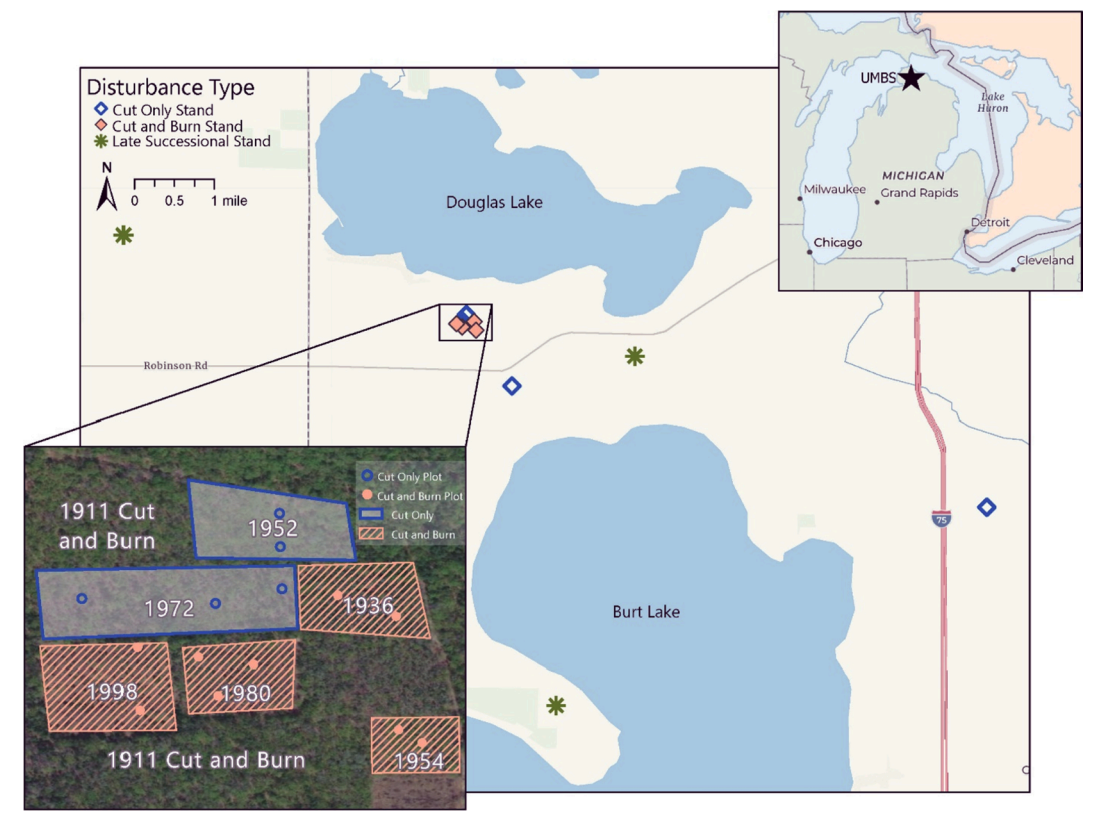


Fig. 1. Map of the study sites, located at the northern tip of the Lower Peninsula of Michigan, United States. Diamonds indicate center points for stands, and circles indicate plot centers for zoomed in plots. Map fully designed by Laura Hickey. (For interpretation of the references to colour in this figure legend, the reader is referred to the web version of this article.)

 Table 1

 Characteristics of the 11 1-ha forest stands, across the two chronosequence treatments and the three late successional stands.

		•	•			
Name	Disturbance History	Year Established	# of plots	Landform	Soils	Dominant tree taxa
Cut and Burn	Twice cut, twice burned	1936	2	high-level plain	sandy Haplorthod	POGR, PIST, ACRU
		1954	2			POGR, QURU, PIST
		1980	3			POGR, QURU, ACRU
		1998	2			POGR, QURU
Cut Only	Twice cut, once burned	1911	3	high-level plain	sandy Haplorthod	POGR, QURU, PIST
		1952	2			QURU, PIST, POGR
		1972	3			POGR, QURU, ACRU
		1987	3			POGR, QURU, ACRU
DBF	Late succession	1850	3	gently sloping moraine	sandy over loamy Haplorthod	TSCA, QURU, ACRU, FAGR
ENF	Late succession	1885	3	low-level plain	sandy over gravelly Haplorthod	PIRE, POGR, BEPA
MIX	Late succession	1885	3	high-level plain	sandy Haplorthod	PIRE, POGR, PIST

Adapted from Wales et al. (2020)

Schmitt and Grigal 1981, Crow and Erdmann 1983, Hocker and Early 1983, Perala and Alban 1993, Ter-Michaelian and Korzukhin, 1997,

Supplement S3). Annual aboveground wood net primary production (NPPaw) was generated for each plot by calculating the difference between an individual tree's biomass in 2019 and 2014 and dividing by 5 to produce an annual average. If the observed dbh of an individual decreased by less than 10% across the 5-yr interval, the tree was assumed not to have grown at all (8% of all trees, 218 of 2852); for live trees with dbh values declining by > 10% between census dates, we assumed a measurement or entry error and dbh increment was inferred from plot- and species-specific relative growth rate (i.e., percent dbh increase per unit time) averages (0.4% of all trees, 10 of 2852). Values were scaled to the hectare and multiplied by the site-specific mean tissue-weighted C fraction of live wood mass of 0.49 to convert from dry mass to C mass (Gough et al. 2013). Belowground wood pools ($\rm M_{bw}$) and belowground wood NPP (NPPbw) were calculated by multiplying

corresponding plot-level above ground $\rm M_{aw}$ and NPP $_{aw}$, respectively, by 0.20 (Cairns et al. 1997). We report above- and below ground wood mass values derived from 2019 census data.

2.3. Fine root net primary production

We used root ingrowth cores to estimate annual fine root production (NPP $_{fr}$) from 2016 through 2019. Cores were 5.35 cm in diameter, 35 cm long, and constructed from PVC mesh tubing. Within each plot, cores were installed at 5, 10, and 15 m along transects at 0°, 120° and 240°, respectively, from the plot center. Cores could not be installed in the ENF stand due to a high seasonal water table and, thus, root primary production was (and, consequently total NPP and NEP were) not estimated for this stand. Prior to installation, A-horizon (averaging 2–3 cm thickness), 0–15 cm and 15–30 cm depth increments were excavated in each plot, sieved using a 4 mm mesh screen within 2 days to remove

coarse fragments and roots, and re-packed into cores within 4 days of initial soil collection. Temporarily removed O-horizon material was placed on top of root-free mineral soil and cores were incubated in the ground from late April/early May to late September/mid-October. Following incubation, ingrowth cores were removed and stored frozen until processed. Fine roots were separated from soil using a 2-mm sieve, dried in an oven at ~ 60 °C, massed, and analyzed for percent C using a Costech Analytical CHN Analyzer in 2016 and 2017 and loss-on-ignition in 2018 and 2019. Samples were adjusted for mineral contamination by the use of percent C analyses in 2016 and 2017, and by the use of a loss on ignition method for 2018 and 2019. Specifically, fine root biomass values were adjusted assuming an average C concentration of 47%, such that each plot-level fine root mass value was scaled down in proportion to its amount of mineral contamination relative to the 47 % C 'clean' criterion. For loss on ignition, mass losses were multiplied by 0.5, assuming half the lost mass was C, to determine % C for each sample. Each plot was scaled to Mg C ha⁻¹ based on the surface area sampled and core sample size.

2.4. Leaf litter and fine debris mass and production

We estimated leaf litter (M_I) and fine debris (M_{fd}) mass production and flux (NPP_I and NPP_{fd}) from litter traps sampled annually from 2012 to 2020. One-meter tall litter traps constructed of window screen material and supported by heavy gauge wire were 1-m deep with a circular surface area of 0.264 m^2 . Three traps were randomly distributed in each plot, although the number periodically varied because of damage. The content of litter traps was collected \sim weekly every autumn until litterfall ceased, combined within a plot, then sorted into fine debris and leaves. Leaf and fine debris mass was scaled to the stand and converted to C mass using a site-specific value of 48% C mass per dry mass (Gough et al. 2007). To estimate the mass of evergreen needles retained by live trees (rather than shed annually), we multiplied litter trap mass by a site-calibrated value of 2.5. We estimated NPP_I and NPP_{fd}, from scaled litter trap values, presenting stand averages across years.

2.5. Coarse woody debris mass and heterotrophic flux

To calculate coarse woody debris mass (Mcwd), a census of downed coarse woody debris (CWD) > 20 cm in length and > 5 cm in diameter was conducted in 2014 and 2020. CWD was sampled in three, 6 m \times 6 m permanent subplots within each plot, which were located at 0°, 120° and 240° azimuths located 6 m from plot center. For each CWD sample, length, as well as diameter at both ends and the midpoint, were recorded and a decay class from 1 (recently fallen, intact bark and wood) to 5 (fully decayed and without structure) was assigned (Marra and Edmonds 1994). Coarse woody debris mass (M_{cwd}) values were calculated using the 2020 census, assuming a cylindrical shape and using species-specific decay class wood densities (Gough et al. 2007). The annual heterotrophic flux from coarse woody debris was calculated by subtracting each plot level 2014 from 2020 values, and dividing by six. Coarse woody debris fluxes counted toward primary production when positive (NPP_{cwd}) and the total heterotrophic flux when negative (R_{cwd}) (Gough et al. 2007). Dry mass was converted to C mass using a site-specific fraction of 0.5 (Gough et al. 2007).

2.6. Soil carbon mass

We estimated total soil C mass (M_s) from 2 to 3 soil profiles excavated from each plot over the course of two days in July 2014. O- and A-horizons were removed as a 225 cm² monolith. Next, the mineral soil was removed using a 5.2 cm internal diameter steel pipe, in depth increments of 0–15, 15–30, 30–60, and 60–100 cm. The O- and A-horizon monoliths were immediately frozen, and processed within 4 months. Mineral soil increments were air dried at 25 °C for 1 week, then sieved to separate into pebbles/gravel (minerals > 2 mm), coarse root (roots > 2

mm diameter), fine root (roots < 2 mm diameter) and fine earth components. All fractions were then oven dried and weighed. The same process was followed in the O- and A- horizon monolith after fibrous organic material was removed from the surface. After drying, fine root samples, fibrous organic material and fine earth were ball milled separately to a powder texture.

O- and A-horizons were analyzed for total C concentrations using a Costech Analytical CHN Analyzer in the UMBS Analytical Laboratory. Mineral soil C concentrations for the four depth increments were determined using a Costech Analytical CHN Analyzer or a PerkinElmer Series II CHNS/O Elemental Analyzer. Total C concentrations for a random subset of n = 10 samples (0.1–0.4 %C) analyzed on both instruments differed by 0.02 – 0.07 %C and were strongly related ($r^2 = 0.98$).

For each plot, M_{oa} was calculated as the product of the soil mass per unit area, C concentration, and an expansion factor to convert to Mg C ha⁻¹. M_{min} was calculated as the product of fine earth total C concentration, soil increment thickness, and bulk density (fine earth divided by core increment volume). M_s is the sum of M_{oa} and M_{min} .

2.7. Bulk and heterotrophic soil respiration

To estimate the annual C flux from bulk soils and from soil heterotrophs only, we collected point measurements of total soil respiration (R_s) and heterotrophic soil respiration (R_{sh}), estimated continuous (i.e., gap-filled) fluxes from temperature-response models, and integrated and scaled to the whole stand to derive annual fluxes. For R_s measurements, PVC soil collars were installed in 2014 to a depth of 3 cm measurements at azimuths of 0°, 72°, 144°, 216°, and 288° and 3, 6, 9, 12, 15 m from the plot center, respectively. For R_{sh}, we installed 80-cm deep trench collars in early July 2020 constructed of schedule 40 PVC tube placed 1 m away from the 0° , 144° and 288° shallow respiration collars within each subplot. Cores were driven vertically into the earth using sledgehammers until the PVC tube cleared the surface of the soil by ~ 3 cm. This method, also known as deep collar trenching, severs roots within the soil column, gradually eliminating autotrophic respiration (Bond-Lamberty et al. 2011). To ensure the attenuation of autotrophic respiration and isolation of R_{sh}, we measured paired surface and trench collars every two days after installation of the latter, until trench collar fluxes were statistically asymptotic (i.e., did not significantly differ between measurement dates), the approximate point at which autotrophic respiration is zero (Fig. S1).

In situ paired R_{sh} and R_s were repeatedly measured during four climatologically distinct periods between: July 28th and August 11th, 2020 (growing season); October 8th and 9th 2020 (beginning of leaf off); November 3rd and 4th (end of leaf-off); and November 16th and November 20th (dormant season). Two measurements were recorded at each collar using a LI-COR LI-6400 paired with a LI-6400–09 soil $\rm CO_2$ flux chamber (LI-COR Inc.). If the sequentially measured fluxes differed by >10%, measurements were repeated until the values fell within 10% of each other. Concurrent with respiration, soil temperature and moisture measurements were taken 2 cm from the edge of each collar at a depth of 7.5 cm and 2.0 cm below the soil surface (Curtis et al. 2005). $\rm R_{s}$ measurements were also recorded periodically between 2014 and 2021 at the same sites, and these measurements were incorporated into the overall $\rm R_{s}$ data collection.

To scale instantaneous point measurements of R_s and R_{sh} to annual C fluxes, we developed temperature-response functions for R_s for each individual plot, utilizing the full 2014–2021 span of R_s data. Separate warm and cold soil temperature models were developed to predict the relationship between temperature and soil respiration. For "cold" temperature measurements (below 9° C), a linear model with zero as the origin was produced for each plot using soil temperature as a predictor of R_s , reflecting the low metabolic rates at freezing (Curtis et al. 2005, Fig. S2). For "warm" soil temperature measurements (above 9° C), a model of the form efflux = a * e^(b * temperature), where a and b are plot

specific parameters, was developed for each plot (Fig. S2). Soil moisture was not a significant predictor of $R_{\rm s}$ and $R_{\rm sh}$, and thus was omitted from our predictive models.

Next, we generated 30-minute, plot-specific soil temperatures from regression models relating point soil temperature measurements to nearby (<15 km distance) continuous measurements from a fixed location, the US-UMB Ameriflux tower (Pastorello et al. 2020). Using 30 min soil temperature estimates, mean annual estimates of soil CO₂ efflux were generated by driving models with plot-specific temperatures from 2014 through 2020 to obtain an average encompassing of climatic variation during the study period.

To derive annual estimates of R_{sh}, we employed multiple independent approaches, acknowledging the high uncertainty associated with this flux at our site (Gough et al. 2007) and elsewhere (Bond-Lamberty et al. 2018). Our first approach ("Method 1", R_{sh1} in Table 3) estimated R_{sh} using paired R_s:R_{sh} values. Generating plot-specific trench collar to shallow collar respiration ratios, with different ratios separately generated from the "growing season" collections (July and August 2020 measurements) and the "dormant season" measurements (October and November 2020 measurements), we multiplied our 30-minute interval estimates of R_s by these field calculated respiration ratios to generate annual estimates of R_{sh}. All 30 min intervals that occurred before day 130 and after day 281 were multiplied by the Dormant Season (D) ratio, and all 30 min intervals occurring in the intervening days were multiplied by the Growing Season (G) ratio. Our second method ("Method 2", R_{sh2} in Table 3) partitioned plot-specific scaled annual R_s fluxes using a global R_{sh}:R_s relationship (Bond Lamberty et al. 2004). Our final method ("Method 3", R_{sh3} in Table 3) applied the mass balance approach of Giardina and Ryan (2002), which assumes a steady-state balance between labile C inputs from leaf and root litter and soil heterotrophic C efflux.

2.8. Carbon pool and flux calculations

For the derivation of carbon pools, fluxes, and their uncertainty, we followed standard approaches for our site that have been cross-validated using independent C flux meteorological towers (Gough et al. 2007, Gough et al. 2008, Gough et al. 2013, Gough et al. 2021). Recognizing the high degree of uncertainty in annual $R_{\rm sh}$ and the sensitivity of the annual net C balance to this large flux, we estimated NEP separately from each of the three $R_{\rm sh}$ estimates. In addition, we inferred the long-term net C balance of chronosequence stands using the C increment (Δ C) approach, which estimates ecosystem net C accumulation or loss from interpolated (between-stand) changes in soil and wood C pool sizes and, over the long-term, is theoretically equivalent to NEP (Gough et al. 2008).

Total soil C (M_s) is the sum of mineral (M_{min}) and organic (M_{oa}) soil mass:

$$M_s = M_{min} + M_{oa}$$

Total ecosystem C mass (M_{total}) is the sum of all above- and belowground (soil and live mass) C pools:

$$M_{total} = M_{aw} + M_{bw} + M_l + M_{fr} + M_{cwd} + M_{min} + M_{oa} \label{eq:model}$$

Total net primary production (NPP) is:

$$NPP = NPP_w + NPP_{cwd} + NPP_{fr} + NPP_1$$

Where NPP_{cwd} is included only when the CWD flux is positive.

Total heterotrophic respiration ($R_h)$ is the sum of R_{sh} estimated using the three approaches described above and negative CWD mass changes:

$$R_h = R_{sh} + |R_{cwd}|$$

Where R_{cwd} is included when the CWD flux is negative. Net ecosystem production (NEP) is:

$$NEP = NPP - R_h \\$$

with each of the three R_h estimates used to derive separate estimates of NEP (NEP₁, NEP₂ and NEP₃, respectively).

The mean annual C increment (Δ C) is:

$$\Delta C = \Delta Maw + \Delta Mbw + \Delta Ms$$

where $\Delta M_{aw},\,\Delta M_{bw}$ and ΔM_s are interpolated from differences in total wood and soil carbon mass between two sequential chronosequence stands.

2.9. Statistical analysis

Standard errors for stand means were generated and analyses were conducted treating the plot as the experimental unit. For model generated estimates of $R_{\rm S}$ and $R_{\rm Sh}$, we generated values on the upper and lower bounds of the 95% confidence band around our model estimates (Curtis et al. 2005). While acknowledging the pseudo-replicated nature of our experimental design and analysis, such an approach is common and remains useful to ecosystem-scale studies for which true replication (e. g., of chronosequences) is not practical (Walker et al. 2010). Compounding standard errors of C pools and fluxes containing multiple terms were estimated as the quadratic sum of component errors (Gough et al. 2007). All analyzes were conducted using R and R Studio software (R Core Team 2021).

Our statistical analysis was intended to address core objectives. For our first objective of assessing the successional trajectories of C pools and fluxes in clear-cut stands established with and without fire, we statistically compared the linear slopes of Cut Only and Cut and Burn age-C pool and -C flux relationships. While acknowledging the potential non-linearity of age-C cycling relationships, we applied more parsimonious linear models because of our limited sample size. When the slope estimates were significant ($\alpha = 0.05$), but not statistically different between chronosequences ($\alpha = 0.05$), we applied a common linear model to data from both chronosequences. For our second objective, we compared the mean values of each of the oldest chronosequence stands to those of the late successional reference stands using ANOVA followed by post-hoc pairwise comparisons via Tukey's HSD ($\alpha = 0.05$). To compare ΔC values, we generated 95% confidence intervals for each measurement period and considered values different from one another when confidence intervals were non-overlapping.

3. Results

3.1. Carbon pools

We observed quantiatively small differences in the successional trajectories of C pools in chronosequence stands with and without fire, with the oldest chronosequence stands storing as much C above- and below-ground as two of three late successional stands (Fig. 2). Total ecosystem C mass accumulated differently in the two chronosequences, increasing by 1.4 Mg C ha $^{-1}$ yr $^{-1}$ in the Cut and Burn and 0.8 Mg C ha $^{-1}$ yr $^{-1}$ in the Cut Only chronosequence across the 89 years of the chronosequence examined; however, the oldest stands in both chronosequences reached an average of \sim 180 Mg C ha $^{-1}$ at roughly the same time because the y-intercept of the Cut and Burn stands was greater than that of the Cut Only, offsetting differences in slope. The total ecosystem C mass of the two oldest chronosequence stands was similar to that of late successional ENF and MIX, which averaged 273 Mg C ha $^{-1}$, but considerably less than DBF's 355 Mg C ha $^{-1}$.

When individual rather than summed C pools were considered, some differences emerged among chronosequences and late successional stands. For example, wood C mass accumulated 55% faster in the Cut and Burn chronosequence than in the Cut Only chronosequence (Table 2). The oldest chronosequence stands and ENF and MIX late successional stands stored similar amounts of wood C, averaging 123 Mg C ha $^{-1}$, while greater wood C storage in the DBF stand of 241 Mg C ha $^{-1}$ accounted for differences in total ecosystem C mass. Other differences

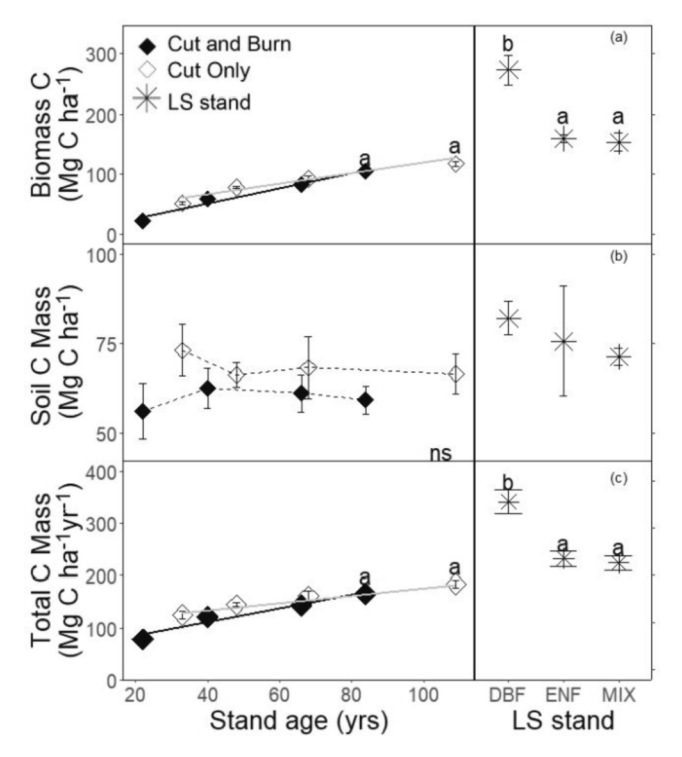


Fig. 2. Total biomass carbon (C, +/- 1 S.E.) (a), soil C mass (b), and total ecosystem (biomass + soil) C mass (c) in Cut Only and Cut and Burn chronosequence and late successional stands. Linear trendlines for each chronosequence are presented when significant, and letters denote significant pairwise differences among late successional stands and the oldest representative chronosequence stands ($\alpha=0.05$). Dotted lines highlight stand connectivity within each chronosequence when no statistical trend is found. "ns"—not significant (in either temporal or pairwise comparisons), LS—Late successional stands, DBF—Deciduous broadleaf forest, ENF—Evergreen needle-leaf forest, and MIX–Mixed deciduous-evergreen forest.

included fine root C mass, which varied more than two-fold, from ~ 4 to 8 Mg C ha $^{-1}$, and was lowest in DBF and MIX stands and highest in the Cut Only chronosequence stands. The CWD-C mass was consistently a small fraction of ecosystem C mass, averaging 1.73 Mg C ha $^{-1}$ (an average of 2% of total ecosystem C mass) across stands, except for the late successional DBF stand, where the CWD pool of 25 Mg C ha $^{-1}$ was nearly ten-fold larger.

In contrast to more variable aboveground C pools, we found total soil C mass was more comparable among chronosequence and late successional stands (Fig. 2). Total soil C mass ranged from 56 in the 1998 Cut and Burn stand to a high of 82 Mg C ha $^{-1}$ in the DBF LS stand, averaging 68 Mg C ha $^{-1}$ across all stands. The mineral soil was consistently the largest belowground C pool, averaging 46 Mg C ha $^{-1}$ across all stands. O-horizon C mass was more variable, averaging 27 Mg C ha $^{-1}$ in the ENF and DBF late successional stands, which was greater than the mean of 18 Mg C ha $^{-1}$ in the chronosequence and MIX stands.

3.2. Carbon fluxes

3.2.1. Net primary production

We did not find a significant linear relationship between total NPP and stand age in either the Cut Only or Cut and Burn chronosequences, and chronosequence stands' total NPP was within the range of the two late successional stands (DBF, MIX) for which production was calculated (Fig. 3). Total NPP averaged 5.11 Mg C ha $^{-1}$ yr $^{-1}$ in the chronosequence stands. Mean differences among stands in total NPP were driven largely by wood NPP, which averaged 1.98 Mg C ha $^{-1}$ yr $^{-1}$ in the chronosequence stands, 3.62 Mg C ha $^{-1}$ yr $^{-1}$ in DBF, and 0.94 Mg C ha $^{-1}$ yr $^{-1}$ in ENF and MIX late successional stands. Fine root NPP exhibited no

significant increase over time or among chronosequence and late successional stands, averaging 1.68 Mg C ha $^{-1}$ yr $^{-1}$ (Table 2). NPP $_{\rm lf}$ and NPP $_{\rm fd}$ did not change significantly over time, as the single point sample sizes at each stand age prevented any type of temporal or pairwise comparisons.

3.2.2. Coarse woody debris fluxes

The net C flux of coarse woody debris was consistent among chronosequence and late successional stands, with the exception of emerald ash borer- and beech bark disease-infested DBF. Mean CWD fluxes in chronosequence stands were negative and thus applied to heterotrophic respiration estimates, averaging -0.015~Mg C $ha^{-1}~\text{yr}^{-1}$. In contrast, CWD fluxes in DBF were positive, with NPP $_{\text{cwd}}$ averaging 3.11 Mg C $ha^{-1}~\text{yr}^{-1}$, indicating a large influx of coarse woody debris.

3.2.3. Bulk and heterotrophic soil respiration

We did not observe significant changes over time in chronosequence R_s values, nor were differences apparent between the oldest chronosequence stands and the late successional stands. Instead, scaled estimates were variable, averaging 9.7 Mg C ha⁻¹ yr⁻¹ study-wide, but with prediction intervals up to $\sim 300\%$ of mean. R_{sh} estimates varied substantial among methods. Method 1 yielded values that increased over time in the Cut and Burn Chronosequence by 0.04 Mg C ha⁻¹ yr⁻¹ per year, but did not change over time in the Cut Only chronosequence (Table 3). R_{sh} average values did not differ between chronosequences and late successional stands, averaging -5.5 Mg C ha⁻¹ yr⁻¹ across both the secondary and late successional stands (Fig. 4). According to Method 2, annual R_{sh} did not change with stand age in the chronosequence stands and values were comparable to those derived from late successional reference stands, averaging 5.1 Mg C ha⁻¹ yr⁻¹ study-wide. Method 3 did not produce temporal or chronosequence-late successional differences either, generating a relatively low study-wide mean at 4.4 Mg C $\mathrm{ha}^{-1}\ \mathrm{yr}^{-1}$.

The estimated fraction of R_{sh} contributing to R_s was variable among stands and seasonally, ranging from a low of 35% in the 1952 Cut Only stand to a high of 76% in the late successional DBF stand during the growing season, and 47% in the late successional ENF and an implausible 109% of R_s in the 1952 stand during the dormant season.

$3.3. \ \ \textit{Net carbon balance: Net ecosystem production and carbon increment}$

Although estimates of net C balance differed depending on the method used, successional trajectories were similar in chronosequences with and without fire, and their NEP values fell within the range of late successional stands. The differences between the three approaches to estimating R_{sh} drove variation in stand-scale NEP, producing estimates of net C balance that ranged from negative (i.e., a C source) to positive (i. e., a C sink) for the same stands (Fig. 5). Our first approach yielded relatively low and often negative NEP and values, while the other two methods produced higher and more similar estimates. Carbon increment-based estimates were made with high uncertainty, but consistently suggest that stands in both chronosequences were comparatively weak C sinks, averaging 1.16 Mg C ha⁻¹ yr⁻¹. Given the high uncertainty associated with these estimates and differences among methods, our net C balance data provide little concrete evidence for different successional patterns in net C balance between Cut Only and Cut and Burn chronosequences, or differences in NEP among the oldest secondary forests and late successional forests (Fig. 5). However, our results show that chronosequence-based successional changes in net C balance are comparable among methods, and they suggest large variability among late successional stands.

3.4. Temporal changes in soil temperatures and fluxes

With R_{sh} values higher and, consequently, NEP values lower than prior site observations (Gough et al. 2008), we compared the soil

Table 2 Mean (+/- 1 S.E.) stand-level carbon pools and fluxes. M_{aw} = above ground wood pool, M_{bw} = below ground wood pool, M_{lf} = leaf pool, M_{fd} = fine debris pool, M_{fr} = fine root pool, M_{cwd} = coarse woody debris pool, M_{oa} = soil organic layer pool, M_{min} = soil mineral layer pool, NPP_{aw} = NPP of aboveground wood, NPP_{bw} = NPP of belowground wood, NPP_{lf} = NPP of leaves, NPP_{fd} = NPP of fine debris, NPP_{fr} = NPP of fine roots, NPP_{cwd}/R_{cwd} = NPP of coarse woody debris/Respiration of coarse woody debris (NPP when positive, Respiration when negative). Error presented parenthetically when available.

	Cut and Bur	n			Cut Only			LS stands				
	Stand age (y	vears)							<u>, </u>			
	22	40	66	84	33	48	68	109	DBF	ENF	MIX	
C Pools												
M_{aw}	12.84	42.47	59.85	80.5	34.13 (2.5)	55.63	67.05	88.28	201.07	123.83	120.34	
	(4.36)	(4.56)	(1.44)	(2.45)		(1.41)	(3.62)	(4.06)	(24.12)	(5.89)	(14.37)	
M_{bw}	2.57	8.49 (0.91)	11.97	16.1	6.83 (0.5)	11.13	13.41	17.66	40.21	24.77	24.07	
	(0.87)		(0.29)	(0.49)		(0.28)	(0.72)	(0.81)	(4.82)	(1.18)	(2.87)	
M_{lf}	0.77	0.98	1.19	1.45	1.18	1.45	1.34	1.61	2.13	3.75	3.06	
M_{fd}	0.12	0.21	0.32	0.39	0.16	0.27	0.27	0.58	0.56	0.38	0.41	
M_{fr}	4.2 (0.52)	6.3 (0.93)	6.75 (0.74)	6.84 (0.46)	8.35 (0.16)	7.88 (1)	9.58 (0.66)	7.94 (0.34)	4.16 (0.79)	7.23 (1.68)	4.61 (0.78)	
M_{cwd}	1.27 (0.86)	0.8 (0.31)	2.55 (1.36)	0.97 (0.56)	1.14 (0.21)	2.45 (0.48)	1.39 (1.1)	1.81 (1.08)	25.14 (3.01)	1.67 (0.97)	3.24 (2.67)	
M_{oa}	16.94	16.62	17.15	15.05	18.51	19.21	20.29	20.78	34.1 (3.51)	37.22 (7.6)	19.61	
ou.	(8.51)	(1.26)	(3.86)	(2.32)	(3.78)	(4.14)	(5.35)	(1.86)			(2.85)	
M_{min}	39.28	45.94 (6)	44.01	44.3	54.66	47.16	48.1 (3.38)	45.79	48.06	38.54	51.77	
	(0.79)		(1.39)	(1.59)	(6.72)	(1.92)	(,	(3.67)	(2.66)	(7.88)	(2.31)	
C Pool Totals			,,	(,	,			()	(,	()	, ,	
Biomass C	21.78	59.26	82.63	106.25	51.79	78.8 (1.82)	93.05	117.88	273.28	161.63	155.73	
	(4.56)	(4.75)	(2.14)	(2.6)	(2.56)	, ,	(3.91)	(4.29)	(24.79)	(6.31)	(14.92)	
Soil C Mass	56.22	62.56	61.16	59.35	73.17	66.37	68.39	66.57	82.16	75.76	71.38	
	(7.72)	(5.61)	(5.26)	(3.91)	(7.21)	(3.37)	(8.73)	(5.51)	(4.66)	(15.4)	(2.38)	
Total C	78 (8.97)	121.81	143.79	165.6	124.95	145.17	161.44	184.45	355.44	237.39	227.11	
Mass	()	(7.36)	(5.67)	(4.7)	(7.65)	(3.83)	(9.57)	(6.99)	(25.22)	(16.64)	(15.11)	
C Fluxes		(, 100)	(0.0.)	()	(,,,,,,	(0.00)	(-10,)	(4177)	(====)	(=====,	()	
NPP _{aw}	0.96 (0.34)	1.79 (0.27)	1.76 (0.15)	1.79 (0.14)	1.73 (0.14)	1.84 (0.14)	1.81 (0.27)	1.5 (0.18)	3.01 (0.42)	0.64 (0.11)	0.92 (0.26)	
NPP_{bw}	0.19 (0.07)	0.36 (0.05)	0.35 (0.03)	0.36 (0.03)	0.35 (0.03)	0.37 (0.03)	0.36 (0.05)	0.3 (0.04)	0.6 (0.08)	0.13 (0.02)	0.18 (0.05)	
NPP_{lf}	0.77	0.96	1.02	1.12	1.06	1.15	1.14	1.12	1.43	1.51	1.41	
NPP _{fd}	0.12	0.21	0.32	0.39	0.16	0.27	0.27	0.58	0.56	0.38	0.41	
NPP _{fr}	1.81	1.77 (0.11)	1.87 (0.25)	1.3 (0.1)	1.92 (0.06)	1.07 (0.06)	2.45 (0.55)	2.18 (0.14)	0.92 (0.18)	-	1.48 (0.15)	
	(0.25)	11,7 (0111)	1107 (0120)	1.0 (0.1)	11,52 (0.00)	1.07 (0.00)	2. 10 (0.00)	2.10 (0.11)	0.52 (0.10)		11.10 (0110)	
NPP _{cwd} /	-0.29	-0.13	0.3 (0.31)	-0.25	0.01 (0.1)	0.22 (0.13)	0.03 (0.17)	0 (0.23)	3.11 (0.11)	0.04 (0.26)	0.48 (0.44)	
R _{cwd}	(0.01)	(0.13)	0.0 (0.01)	(0.13)	3.01 (0.1)	0.22 (0.10)	0.00 (0.17)	0.20)	0.11 (0.11)	0.01 (0.20)	3. 10 (0.14)	
C Flux Totals		(3.10)		(0.10)								
NPP	3.86	5.1 (0.3)	5.33 (0.29)	4.96	5.23 (0.15)	4.7 (0.16)	6.04 (0.62)	5.69 (0.23)	6.53 (0.46)	_	4.4 (0.3)	
	(0.43)	0.1 (0.0)	0.00 (0.2)	(0.17)	3.20 (0.13)	(0.10)	0.01(0.02)	0.05 (0.20)	0.00 (0.10)		1 (0.0)	

temperatures from a prior assessment in 2004 (Gough et al. 2007) with those used to model R_{sh} in the present study, asking whether such differences account for lower apparent NEP. Soil temperature means generated using the same methods were similar but statistically different between current and prior study periods, averaging 7.7 and 8.0 $^{\circ}\text{C}$ in the Gough et al. 2007 and this manuscript, respectively; however, temperature extremes were more abundant during our recent study period, with a larger fraction of half-hourly (this study) or hourly (Gough et al. 2007) temperatures below 0 $^{\circ}\text{C}$ and higher than 15 $^{\circ}\text{C}$ in our current analysis (Fig. 6). Because of the exponential relationship between soil temperature and R_{s} , the higher number of + 15 $^{\circ}\text{C}$ temperature observations during our study period resulted in annual R_{s} estimates that were 72% or 2.56 Mg C ha $^{-1}$ higher than those reported for 2004.

4. Discussion

We did not find support for the hypothesis that fire after clear-cut harvesting lowers the successional trajectory of C pools and fluxes in Great Lakes aspen-dominated forests. Instead, stands that were clear-cut harvested only vs. those that were clear-cut and burned exhibited similar successional changes in most individual pools and total C mass, and in major fluxes, including total NPP and heterotrophic soil respiration, and, thus, net C balance or NEP. Even though different approaches produced quantitatively different net C balance values, they yielded similar temporal patterns. While we hypothesized that fire-associated N losses (White et al. 2004) would depress the successional trajectory of C

pools and fluxes, biome and global meta-analyses show that C pools depleted by fire can rebound rapidly, particularly in deciduous forests subjected to slash- rather than crown-fueled fires (Nave et al. 2011, Li et al. 2021). Moreover, C pool and flux trajectories following fire are highly variable among forest types (Amiro et al. 2010) and ecoregions (Amiro et al. 2001), and aspen-dominated forests such as ours may recover C pools (Alexander and Mack 2016) and fluxes (Peters et al. 2013) more rapidly after fire than evergreen needleleaf forests. In established aspen stands, a clonal network of carbohydrate-rich roots may fuel prolific resprouting following fire (Smith et al. 2011), a disturbance-adapted response that may have supported comparable recovery in chronosequences with or without fire. Importantly, this interpretation reinforces findings that ecosystems containing fireadapted species may be more functionally resilient to fire (Johnstone et al. 2016), and suggests that non-fire adapted forests in the upper Great Lakes and elsewhere might respond with less resilience to the addition of

We also found limited evidence for the hypothesis that fire following clear-cut harvesting limits the recovery of C pools and fluxes to levels below those of our reference late successional forests. Although C pools and fluxes were variable among late successional forests, both the Cut Only and Cut and Burn stands generally possessed values that were within or approaching the range of older legacy stands, suggesting that stand-replacement had a limited effect or, when it did, the recovery of C cycling processes had already occurred or was underway prior to our data collection. For example, total soil C mass was comparable among

Table 3

Total annual soil respiration (R_s) and total heterotrophic respiration values generated via three different methods: the exponential model method (R_{h1}), a method utilizing a global relationship between total and heterotrophic soil respiration (R_{h2}), and the Labile carbon method (R_{h3}), outlined in Giardina and Ryan (2002) and described above. The corresponding NEP values generated from these three different methods are displayed as NEP₁, NEP₂ and NEP₃, respectively. Values are divided into Dormant Season (D), Growing Season (GS) and Annual (A) values when possible. All metrics are given in units of Mg C ha⁻¹ yr⁻¹, and the 95% upper and lower bounds of the models used to generate these metrics are displayed in parentheses.

	Cut and	l Burn		Cut Only											
	Stand a	ige (yeai	rs)												
	22			40			66			84			33		
Season R _s	D -1.18	GS -8.9	A -10.08 (-35.93, 0)	D -1.28	GS -8.03	A -9.31 (-21.45, -1.65)	D -1.56	GS -8.23	A -9.8 (-25.64, 0)	D -1.48	GS -7.88	A -9.35 (-21.29, -1.39)	D -1.48	GS -8.15	A -9.63 (-24.66, -0.54)
R _{h1}	-0.9	-3.91	-4.81 (-20, 0)	-1.15	-3.79	-4.94 (-12.17, -0.14)	-0.87	-4.36	-5.23 (-13.75, 0)	-1.17	-5.78	-6.95 (-15.81, -1.01)	-1.09	-4.03	-5.12 (-13.79, -0.03)
R _{h2}	-1.1	-4.82	-5.27 (-8.64, 0)	-1.17	-4.47	-4.97 (-6.05, -0.2)	-1.35	-4.55	-5.16 (-6.6, 0)	-1.3	-4.41	-4.99 (-7.33, -0.97)	-1.3	-4.52	-5.1 (-6.62, -0.05)
R_{h3}	-	-	-4.18 (0.5)	-	-	-4.33 (0.32)	-	-	-4.5 (0.38)	-	-	-4.25 (0.2)	-	-	-4.45 (0.16)
NPP	-	-	3.86 (0.43)	-	-	5.1 (0.3)	-	-	5.33 (0.29)	-	-	4.96 (0.17)	-	-	5.23 (0.15)
NEP_1	-	-	-1.24 (-20.43, 0.43)	-	-	0.03 (-12.5, 0.19)	-	-	0.1 (-14.18, 0.43)	-	-	-2.25 (-16.03, -0.79)	-	-	0.05 (-13.97, 0.15)
NEP_2	-	-	-1.7 (-9.07, 0.43)	-	-	-0.01 (-6.38, 0.13)	-	-	0.17 (-7.03, 0.43)	-	-	-0.29 (-7.55, -0.75)	-	-	0.08 (-6.8, 0.13)
NEP_3	-	-	-0.62 (0.5)	-	-	0.63 (0.32)	-	-	0.83 (0.38)	-	-	0.45 (0.2)	-	-	0.72 (0.16)
Delta C	-	-	_	_	-	2.3 (5.34)	_	-	0.82 (3.54)	-	_	1.19 (3.38)	-	-	_

the oldest chronosequence stands and late successional stands, with the exception of the more C-rich DBF stand. Additionally, C stored in the wood mass of clear-cut only and clear-cut and burned stands was on a sharp upward trajectory over time; these successional patterns suggest sustained high rates of wood production in secondary forests could support continued recovery of wood C mass pools into the future. Such findings should be interpreted with caution, however, because late successional and chronosequence stands were sometimes positioned on different landforms and soils, and therefore, the former should not be considered developmental end-members of the latter. Instead, our findings highlight the comparably high C storage of older secondary and late successional forest stands, despite different disturbance histories, landforms, soils, and vegetation. Comparable C pool and flux profiles in ecologically different forests has been noted for other forested land-scapes, but is not universal (Birdsey 1992).

A lower C cycling successional trajectory and recovery was anticipated following fire because aspen-dominated secondary forests at our site are N-limited (Nave et al. 2009) and fire in the Cut and Burn stands diminished long-term N availability (White et al. 2004, Nave et al. 2019). Fire in the Cut and Burn stands reduced soil ammonium-N by half (Nave et al. 2019), but our study shows this decline was not enough to limit the rate and magnitude of regrowth. Although not expected, this finding is consistent with that of a global meta-analysis concluding that deciduous broadleaf forests subjected to low fire frequencies recover to pre-disturbance production rates quickly, particularly when N losses are not severe (Li et al. 2021). However, a number of additional factors that we did not characterize in our analysis could determine C cycling responses to fire. These include: the plant functional type(s) affected by disturbance (Peters et al. 2013), fire severity (Li et al. 2021), the degree of fire adaptation of resident species (Cai et al. 2018), and the quantity and type of biotic and abiotic material legacies remaining after fire (Johnstone et al. 2016). At our site, vigorous aspen resprouting after fire may have supported rapid recovery (Gough et al. 2007) despite these N losses, while the recruitment of mid-late successional tree species (Fahey

et al. 2016, Shiklomanov et al. 2020), and accumulation of biodiversity (Gough et al. 2010) and canopy complexity (Hardiman et al. 2013, Scheuermann et al. 2018) – with or without fire – may sustain forest production into mid-late stages of secondary succession.

A notable finding outside of our core objectives was that latesuccessional forests can serve as considerable long-term stores of carbon, retaining large quantities of C in biomass and soil. Although such side-by-side comparisons are rare because late successional communities often do not co-exist on cutover landscapes, our findings reaffirm synthesis studies showing that late successional forests can be large reservoirs of stored C and, in some cases, may persist as C sinks (Luyssaert et al. 2008, Curtis and Gough 2018, Besnard et al. 2018). Of particular note is the deciduous broadleaf forest positioned on a nutrient-rich mesic site, which stored > 40% more C in biomass and soils than other late successional stands and was the strongest net C sink among all (secondary and late successional) stands. In contrast, the mixed and pine-dominated late successional stands' NPP was comparable to or lower than that of secondary stands, suggesting that their production is plateauing or past peak. This finding can inform the role of forestry in promoting C benefits across the region's managed forest landscapes, e.g., by indicating that longer rotation lengths or harvest reserves may be more appropriate in mesic deciduous than xeric coniferous forests (Nave et al., 2017, Ontl et al., 2020).

Whether the late successional deciduous broadleaf forest continues to take up and store large amounts of C will likely depend on the longer-term effects of ongoing emerald ash borer and beech bark disease (Flower et al. 2013, Morin et al. 2007). Within the past decade, insect pests have increased tree mortality and transferred a large fraction of trees from live to dead C pools. This is evidenced in the order-of-magnitude greater woody debris pool size, which could signal a progressive reduction in live vegetation available to fix carbon (Clark et al. 2018) and increase respiratory-C from decomposition (Harmon et al. 2011). Observations in nearby secondary forests suggest compensatory C uptake and growth by healthy, live vegetation together with slower-

Cut Only										LS stands										
Stand a	Stand age (years)																			
48			68			109			DBF			ENF			MIX					
D	GS	A	D	GS	A	D	GS	A	D	GS	A	D	GS	A	D	GS	A			
-1.43	-8.09	-9.51 (-23.3, -0.95)	-1.33	-9.2211	-10.55 (-23.41, -2.36)	-1.18	-8.46	-9.64 (-27.13, -0.43)	-1.52	-7.08	-8.6 (-28.69, 0)	-2.35	-8.16	-10.52 (-26.75, -0.55)	-1.79	-7.73	-9.52 (-28.38, 0)			
-1.33	-4.18	-5.5 (-14.3, 0)	-0.78	-3.80834	-4.59 (-10.54, -0.65)	-0.89	-4.13	-5.02 (-14.74, 0)	-1.31	-4.99	-6.3 (-22.42, 0)	-1.27	-4.43	-5.7 (-14.42, -0.24)	-1.56	-4.77	-6.33 (-19.68, 0)			
-1.27	-4.49	-5.04 (-6.81, 0)	-1.2	-4.94459	-5.46 (-5.45, -0.62)	-1.1	-4.64	-5.1 (-6.96, 0)	-1.33	-4.08	-4.68 (-9.28, 0)	-1.83	-4.52	-5.44 (-6.85, -0.3)	-1.5	-4.35	-5.06 (-8.6, 0)			
-	-	-4.06 (0.17)	-	-	-4.9 (0.83)	-	-	-4.9 (0.27)	-	-	-4.31 (0.49)	-	-	-	-	-	-4.55 (0.34)			
-	-	4.7 (0.16)	-	-	6.04 (0.62)	-	-	5.69 (0.23)	-	-	6.53 (0.46)	-	-	-	-	-	4.4 (0.3)			
-	-	-0.8 (-14.5, 0.2)	-	-	1.38 (-11.18, -0.01)	-	-	0.53 (-15.07, 0.33)	-	-	0.23 (-22.89, 0.47)	-	-	-3.18 (NA, NA)	-	-	-1.93 (-20.22, 0.54)			
-	-	-0.34 (-7.01, 0.2)	-	-	0.51 (-6.09, 0.02)	-	-	0.44 (-7.29, 0.33)	-	-	1.85 (-9.75, 0.47)	-	-	-2.91 (NA, NA)	-	-	-0.66 (-9.14, 0.54)			
-	-	0.65 (0.17)	-	-	1.07 (0.83)	-	-	0.64 (0.27)	-	-	2.22 (0.49)	-	-	-	-	-	-0.15 (0.34)			
-	-	1.35 (4.3)	-	-	0.73 (4.49)	_	_	0.59 (3.62)	-	-	-	_	_	-	_	_	-			

than-expected rates of woody debris decomposition could sustain or minimize declines in C uptake and storage (Stuart-Haentjens et al. 2015, Schmid et al., 2016, Gough et al. 2021). However, whether similar stabilizing mechanisms apply to late successional forests containing different and older tree species assemblages and canopy structures is not known, and is a focus of ongoing investigation.

In addition to uncertainty imposed by biotic disturbances, we found preliminary evidence that an increase in temperature extremes rather than in mean temperature may be gradually eroding the C sink longsupplied by forests at our site. Prior meteorological and inventorybased estimates of NEP for our secondary aspen forests (Gough et al. 2007, 2008ab, 2013, 2021) suggest these ecosystems have been modest but continuous net C sinks for over a century. The lower, including negative, NEP values that we report could be an artifact, associated with sensitivity of a highly uncertain flux to the method of derivation (Philips et al. 2016). However, our comparison of R_{sh} derived from half-hourly soil temperature distributions in 2004 (Gough et al. 2007) and 2014-2020 illustrates that relatively small changes in soil microclimate can have disproportionately greater effects on respiratory C fluxes, which increase exponentially at higher temperatures. In our example, soil temperature means were the same between study periods, but a greater number of high temperature observations forced an increase in R_{sh}, which, in some cases, sufficiently tipped NEP estimates from C sink to source. This subtle but ecologically significant signal of climate change is consistent with predictions of greater temperature extremes (Seneviratne et al. 2012) and globally rising heterotrophic soil respiration (Bond-Lamberty et al. 2018). Whether forests at our site are on the cusp of transitioning to stronger C sources, however, remains unclear given the uncertainty of our net C balance estimates. What's more, a study published in 2017 at the same sites found significantly lower soil temperatures and total soil respiration within the late successional reference stands, indicating that continued and consistent examination of how these forests may be following different carbon storage trajectories is critical in understanding what role they play in the carbon cycle (Liebman et al. 2017). This highlights the value of continuous long-term observations from multiple independent observational platforms and spatial scales (Franklin 1989, Lindenmayer et al. 2012, Lepistö et al. 2014, Giron-Nava et al. 2017).

Higher than expected in-situ R_{sh} rates, discrepancies among net C balance values (i.e. NEP vs. C increment), and large uncertainties in C pools and fluxes underscore several known limitations associated with inventory-based C accounting. Elevated, and sometimes impossibly high (R_{sh} > R_s) in situ heterotrophic respiration values resulted in NEP values that are much lower than those observed in nearby stands using inventory and meteorological tower-based approaches (Gough et al. 2007, 2008, 2013). With estimated heterotrophic respiration unrealistically exceeding total soil respiration in some instances, and overall annual R_h values higher than expected given the carbon inputs in this system, it is evident that some component of the C cycle is being over- or underestimated by the methods used. In contrast, mean C increment values of 1.16 Mg C ha⁻¹ yr⁻¹ in the chronosequence stands are comparable to independent estimates of NEP from our site and others in the region (Gough et al. 2007, 2008, 2013, Bond-Lamberty et al. 2004). In situ estimates of R_{sh} and R_s, particularly when modeled and scaled, are sensitive to anomalous climate, statistical outliers, and oversimplification of a relatively complex ecosystem dynamic. Soil C and efflux are highly spatially variable across multiple ecosystem types including forests (Conant et al. 2003), and thus high certainty estimations of both these features via in situ measurements can be difficult, especially when taken over the course of only one calendar year. Moreover, while chronosequences provide a uniquely powerful tool for examining long-term ecological change through space-for-time substitution, caution must be taken when drawing inferences because of the lack of true treatment replication, the limited area of manipulation, changing environmental and atmospheric conditions over time, and potentially co-varying and thus confounding site and treatment factors (Bond-Lamberty et al. 2004). For example, our relatively small treatment areas (~1 ha) did not replicate the large spatial extent of the

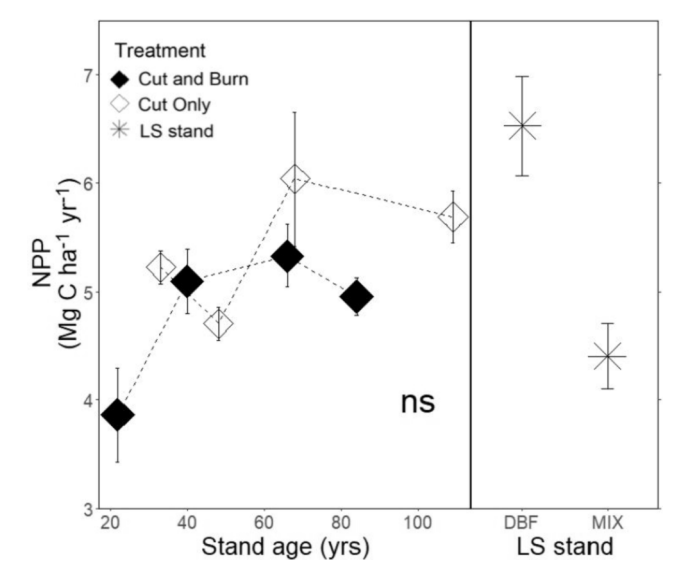


Fig. 3. Total net primary production (NPP) in the Cut Only and Cut and Burn chronosequences and the late successional stands. Linear trendlines for each chronosequence are presented when significant, and letters denote significant pairwise differences among late successional stands and the oldest representative chronosequence stands ($\alpha=0.05$). "ns"– not significant (in either temporal or pairwise comparisons), DBF–Deciduous broadleaf forest and MIX–Mixed deciduous-evergreen forest. Dotted lines highlight stand connectivity within each chronosequence when no statistical trend is found.

region-wide clear-cut harvesting and fires that occurred in the early 20th century and, therefore, our stands were more likely influenced by microclimatic and seed-tree edge effects than larger contiguous disturbances. Our in situ $R_{\rm sh}$ estimates, derived from deep collar trenching, may have underrepresented the effects of root exudates and mycorrhizal production (Bond-Lamberty et al. 2011). Given our anomalously high in situ $R_{\rm sh}$ values, future work will incorporate alternate estimates of this highly uncertain flux, derived from continuous soil C flux measurements and further constrained by independent meteorological-tower based estimates of ecosystem respiration.

5. Conclusion

We conclude that that the successional dynamics and extent of recovery of C pools and fluxes are similar for clear-cut, and clear-cut and burned aspen-dominated forests included in our study, a forest type that is broadly represented in the upper Great Lakes region (Nave et al. 2017). Moreover, these regrown forests are approaching or have already reached the C cycling status of late-successional forests on the same landscape. Our findings provide a useful data point for an underrepresented ecosystem in which fire extent peaked over a century ago, rather than in recent years. Our results have important management implications for the region's forests, demonstrating that fire on aspen-dense Great Lakes landscapes impose few lasting effects on C pools and fluxes. If such biogeochemical effects of disturbance are short-lived (White et al. 2004, Gough et al. 2007, Nave et al. 2019), increased fire frequency in the region (Moritz et al. 2012) may not be detrimental to the future C storage of aspen-dominated forests, but whether such fire tolerance extends to the region's forests with few fire-adapted species is not guaranteed and, in fact, may be unlikely (Johnstone et al. 2016). However, our findings also provide a glimpse into a potential future in which elevated soil C emissions resulting from more abundant temperature extremes overrides the beneficial effects of sustained high NPP, thereby diminishing the C sink status of the region's forests. While model analysis from our site suggests C cycling recovery is highly dependent upon climate (Dorheim et al. 2022), continued field observations are necessary to evaluate and interpret interactions between

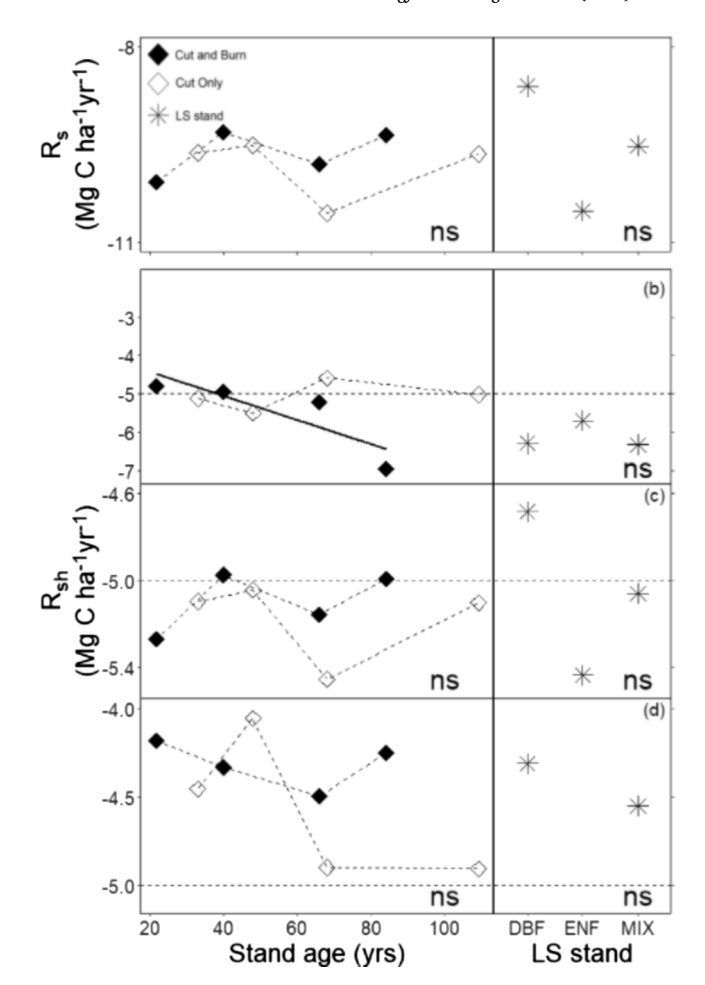


Fig. 4. Total (R_s) and Heterotrophic soil respiration (R_{sh}) in Cut Only and Cut and Burn chronosequences and late successional stands (Deciduous Broadleaf Forest, ENF = Evergreen Needle-Leaf Forest, MIX = Deciduous Broadleaf and Evergreen Needle-Leaf Forest), using the exponential method (3a), global total: heterotrophic soil respiration ratio (3b), and mass balance approach (3c). Linear trendlines are presented when significant (black = Cut and Burn trendline, gray = Cut Only trendline), and letters denote significant pairwise differences among late successional stands and the oldest representative chronosequence stands (α = 0.05). "ns" – not significant (in either temporal or pairwise comparisons. Dotted lines highlight stand connectivity within each chronosequence when no statistical trend is found. Error around points displayed in Table 3. Line drawn at –5 to allow for cross R_h method comparison.

climate, disturbance, and succession, and to develop informed adaptive C management strategies.

Data and code availability: Data and code available at https://portal.edirepository.org/nis/mapbrowse?scope=edi&identifier=243.

CRediT authorship contribution statement

Cameron Clay: Conceptualization, Methodology, Software, Validation, Formal analysis, Investigation, Resources, Data curation, Writing – original draft, Writing – review & editing, Visualization, Project administration. Luke Nave: Conceptualization, Methodology, Validation, Formal analysis, Investigation, Resources, Data curation, Writing – original draft, Writing – review & editing, Supervision, Project administration, Funding acquisition. Knute Nadelhoffer: Conceptualization, Methodology, Validation, Investigation, Resources, Data curation, Writing – review & editing, Supervision, Project administration, Funding acquisition. Christoph Vogel: Resources, Data curation, Writing – review & editing, Project administration. Brooke Propson: Methodology, Validation, Investigation, Resources, Data curation, Writing –

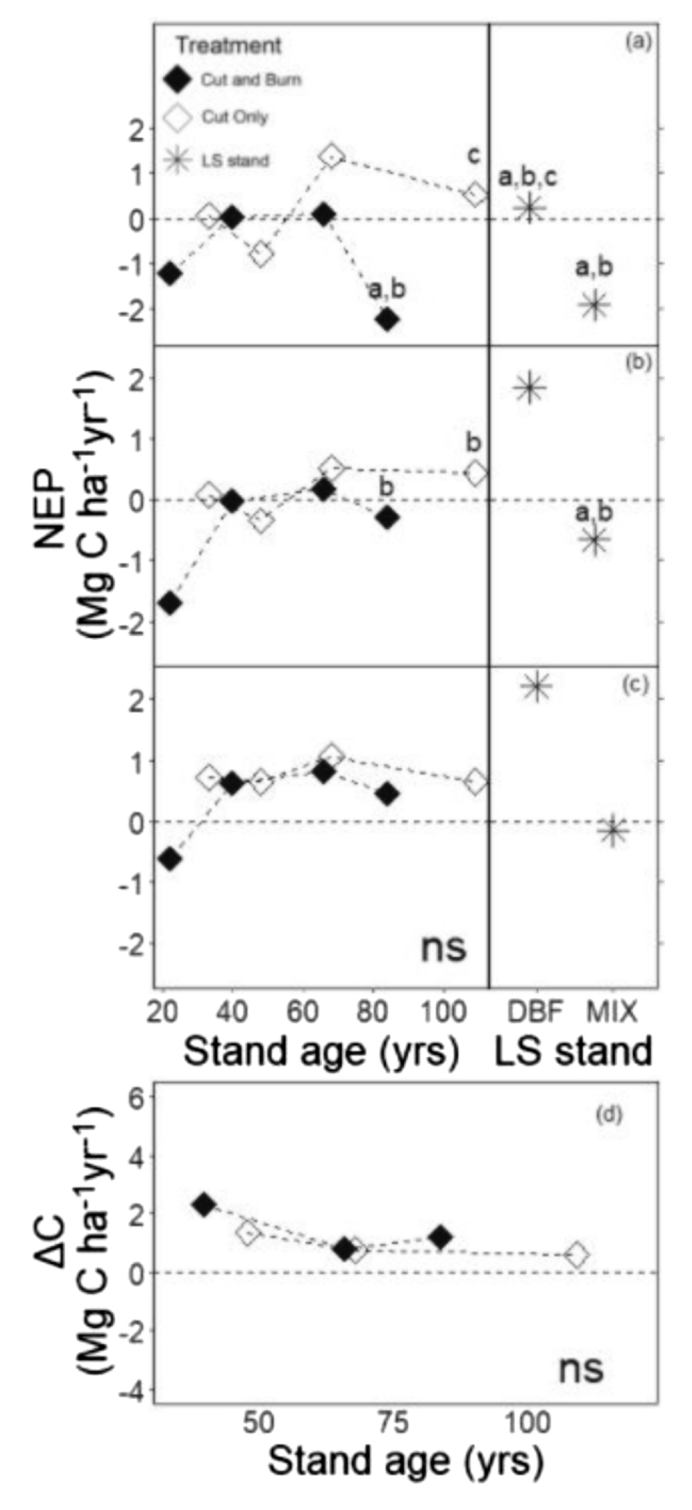


Fig. 5. Net ecosystem production estimates generated via three different R_{sh} modeling approaches in the chronosequence (22 to 109 years old) and late successional plots (DBF = Deciduous Broadleaf Forest, MIX = Deciduous Broadleaf and Evergreen Needle-Leaf Forest). "ns" denotes non-significance in pairwise comparisons between old chronosequence stands and late successional stands, as well as non-significance in temporal trends in the chronosequence. NEP data are not reported for the ENF stand due to the lack of Fine Root data. "ns" denotes non-significance in pairwise comparisons between old chronosequence stands and late successional stands, as well as non-significance in temporal trends in the chronosequence. For illustrative clarity, we omit error bars and refer readers to Table 2.

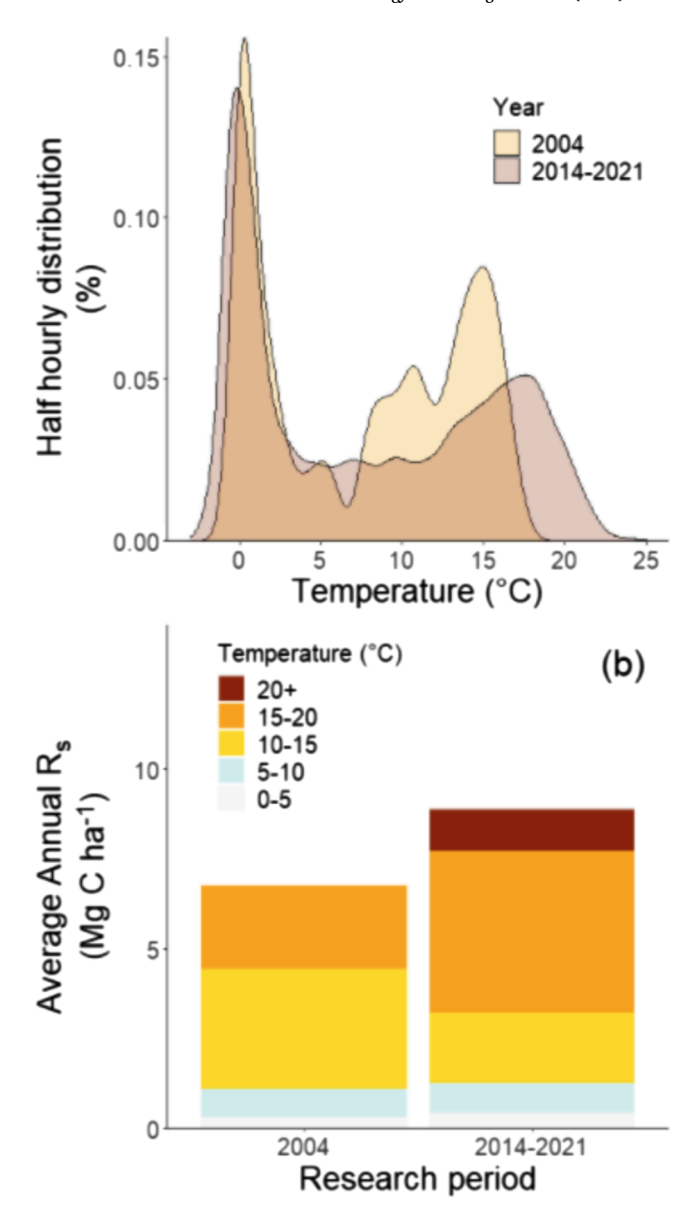


Fig. 6. The half-hourly soil temperature distribution for Gough et al. (2007, Year = 2004) and this paper manuscript (2014–2021) (a), along with their influence on scaled 5 $^{\circ}$ C R_s increments (b). (For interpretation of the references to colour in this figure legend, the reader is referred to the web version of this article.)

review & editing, Project administration. John Den Uyl: Methodology, Validation, Investigation, Resources, Data curation, Writing – review & editing, Project administration. Laura J. Hickey: Methodology, Validation, Investigation, Resources, Writing – review & editing, Visualization. Alexandra Barry: Methodology, Investigation, Writing – review & editing. Christopher M. Gough: Conceptualization, Methodology, Validation, Formal analysis, Investigation, Resources, Data curation, Writing – review & editing, Visualization, Project administration, Funding acquisition.

Declaration of Competing Interest

The authors declare that they have no known competing financial interests or personal relationships that could have appeared to influence the work reported in this paper.

Acknowledgements

This work was supported by the National Science Foundation, Award Nos. DEB-1353908, DEB-1856319, DEB-1127250, and AGS-1262634. We thank the University of Michigan Biological Station for logistical, infrastructure, and personnel support. We thank Kayla Mathes, Kerstin Niedermaier, and Lisa Haber for advising on figures and respiration model structure. We thank Dr. David Edwards for advising on statistical methods.

Appendix A. Supplementary material

Supplementary data to this article can be found online at https://doi.org/10.1016/j.foreco.2022.120301.

References

- Alexander, H.D., Mack, M.C., 2016. A canopy shift in interior alaskan boreal forests: consequences for above- and belowground carbon and nitrogen pools during postfire succession. Ecosystems 19 (1), 98–114. https://doi.org/10.1007/S10021-015-9920-7/TABLES/7
- Amiro, B.D., Barr, A.G., Barr, J.G., Black, T.A., Bracho, R., Brown, M., Chen, J., Clark, K. L., Davis, K.J., Desai, A.R., Dore, S., Engel, V., Fuentes, J.D., Goldstein, A.H., Goulden, M.L., Kolb, T.E., Lavigne, M.B., Law, B.E., Margolis, H.A., Martin, T., McCaughey, J.H., Misson, L., Montes-Helu, M., Noormets, A., Randerson, J.T., Starr, G., Xiao, J., 2010. Ecosystem carbon dioxide fluxes after disturbance in forests of North America. J. Geophys. Res. Biogeosci. 115 https://doi.org/10.1029/2011.010.01390
- Atkins, J.W., Bond-Lamberty, B., Fahey, R.T., Haber, L.T., Stuart-Haëntjens, E., Hardiman, B.S., LaRue, E., McNeil, B.E., Orwig, D.A., Stovall, A.E.L., Tallant, J.M., Walter, J.A., Gough, C.M., 2020. Application of multidimensional structural characterization to detect and describe moderate forest disturbance. Ecosphere 11 (6), e03156. https://doi.org/10.1002/ecs2.3156.
- Besnard, S., Carvalhais, N., Arain, M.A., Black, A., de Bruin, S., Buchmann, N., Cescatti, A., Chen, J., Clevers, J.G.P.W., Desai, A.R., Gough, C.M., Havrankova, K., Herold, M., Hörtnagl, L., Jung, M., Knohl, A., Kruijt, B., Krupkova, L., Law, B.E., Lindroth, A., Noormets, A., Roupsard, O., Steinbrecher, R., Varlagin, A., Vincke, C., Reichstein, M., 2018. Quantifying the effect of forest age in annual net forest carbon balance. Environ. Res. Lett. 13 (12), 124018.
- Birdsey, R.A., 1992. Carbon storage and accumulation in United States forest ecosystems. USDA Forest Service. Gen. Tech. Rep. WO-59. Washington, DC.
- Birdsey, R., Pregitzer, K., Lucier, A., 2006. Forest Carbon Management in the United States. J. Environ. Qual. 35 (4), 1461–1469. https://doi.org/10.2134/jeq2005.0162.
- Bond-Lamberty, B., Wang, C., Gower, S.T., 2004. Net primary production and net ecosystem production of a boreal black spruce wildfire chronosequence. Glob. Change Biol. 10 (4), 473–487. https://doi.org/10.1111/j.1529-8817.2003.0742.x.
- Bond-Lamberty, B., Bronson, D., Bladyka, E., Gower, S.T., 2011. A comparison of trenched plot techniques for partitioning soil respiration. Soil Biol. Biochem. 43 (10), 2108–2114. https://doi.org/10.1016/j.soilbio.2011.06.011.
- Bond-Lamberty, B., Bailey, V.L., Chen, M., Gough, C.M., Vargas, R., 2018. Globally rising soil heterotrophic respiration over recent decades. Nature 560 (7716), 80–83.
- Cai, W.H., Liu, Z., Yang, Y.Z., Yang, J., 2018. Does environment filtering or seed limitation determine post-fire forest recovery patterns in boreal larch forests? Front. Plant Sci. 9, 1318. https://doi.org/10.3389/FPLS.2018.01318/BIBTEX.
- Cairns, M.A., Brown, S., Helmer, E.H., Baumgardner, G. A., Cairns, M.A., Brown, S., Helmer, E.H., Baumgardner, G.A., 1997. Root biomass allocation in the world's upland forests. In *Oecologia* (Vol. 111, Issue 1 ± 11). Springer-Verlag. https://doi.org/10.1007/s004420050201.
- Certini, G., 2005. Effects of fire on properties of forest soils: a review. Oecologia 143 (1), 1-10.
- Clark, K.L., Renninger, H.J., Skowronski, N., Gallagher, M., Schäfer, K.V.R., 2018. Decadal-scale reduction in forest net ecosystem production following insect defoliation contrasts with short-term impacts of prescribed fires. Forests 9 (3). https://doi.org/10.3390/F9030145.
- Conant, R.T., Smith, G.R., Paustian, K., 2003. Spatial Variability of Soil Carbon in Forested and Cultivated Sites. J. Environ. Qual. 32 (1), 278–286. https://doi.org/ 10.2134/jeq2003.2780.
- Crow, T.R., Erdmann, G.G., 1983, Weight and volume equations and tables for red maple in the Lake States. US Forest Service Research Paper, NC-242, 14. https://doi.org/ 10.2737/NC-RP-242.
- Curtis, P.S., Vogel, C.S., Gough, C.M., Schmid, H.P., Su, H.B., Bovard, B.D., 2005.
 Respiratory carbon losses and the carbon-use efficiency of a northern hardwood forest, 1999–2003. New Phytol. 167 (2), 437–456. https://doi.org/10.1111/J.1469-8137.2005.01438.X.
- Curtis, P.S., Gough, C.M., 2018. Forest aging, disturbance and the carbon cycle. New Phytol 219 (4), 1188–1193.
- Fahey, R.T., Stuart-Haëntjens, E.J., Gough, C.M., de La Cruz, A., Stockton, E., Vogel, C.S., Curtis, P.S., 2016. Evaluating forest subcanopy response to moderate severity disturbance and contribution to ecosystem-level productivity and resilience. For. Ecol. Manage. 376, 135–147. https://doi.org/10.1016/J.FORECO.2016.06.001.

- Flower, C.E., Knight, K.S., Gonzalez-Meler, M.A., 2013. Impacts of the emerald ash borer (Agrilus planipennis Fairmaire) induced ash (Fraxinus spp.) mortality on forest carbon cycling and successional dynamics in the eastern United States. Biol. Invasions 15 (4), 931–944. https://doi.org/10.1007/S10530-012-0341-7/FIGURES/5.
- Franklin, J.F., 1989. Importance and Justification of Long-Term Studies in Ecology. In: Likens, G.E. (Ed.), Long-Term Studies in Ecology. Springer, New York, NY. https://doi.org/10.1007/978-1-4615-7358-6_1.
- Giardina, C.P., Ryan, M.G., 2002. Total belowground carbon allocation in a fast-growing Eucalyptus plantation estimated using a carbon balance approach. Ecosystems 5 (5), 487–499. https://doi.org/10.1007/s10021-002-0130-8.
- Giron-Nava, A., James, C.C., Johnson, A.F., Dannecker, D., Kolody, B., Lee, A., Nagarkar, M., Pao, G.M., Ye, H., Johns, D.G., Sugihara, G., 2017. Quantitative argument for long-term ecological monitoring. Mar. Ecol. Prog. Ser. 572, 269–274. https://doi.org/10.3354/MEPS12149.
- Gough, C.M., Vogel, C.S., Harrold, K.H., George, K., Curtis, P.S., 2007. The legacy of harvest and fire on ecosystem carbon storage in a north temperate forest. Glob. Change Biol. 13 (9), 1935–1949. https://doi.org/10.1111/j.1365-2486.2007.01406. x.
- Gough, C.M., Vogel, C.S., Schmid, H.P., Curtis, P.S., 2008. Controls on annual forest carbon storage: Lessons from the past and predictions for the future. Bioscience 58 (7), 609–622. https://doi.org/10.1641/B580708.
- Gough, C.M., Vogel, C.S., Hardiman, B., Curtis, P.S., 2010. Wood net primary production resilience in an unmanaged forest transitioning from early to middle succession. For. Ecol. Manage. 260 (1), 36–41. https://doi.org/10.1016/J.FORECO.2010.03.027.
- Gough, C.M., Hardiman, B.S., Nave, L.E., Bohrer, G., Maurer, K.D., Vogel, C.S., Nadelhoffer, K.J., Curtis, P.S., 2013. Sustained carbon uptake and storage following moderate disturbance in a Great Lakes forest. Ecol. Appl. 23 (5), 1202–1215. https://doi.org/10.1890/12-1554.1.
- Gough, C.M., Curtis, P.S., Hardiman, B.S., Scheuermann, C.M., Bond-Lamberty, B., 2016. Disturbance, complexity, and succession of net ecosystem production in North America's temperate deciduous forests. Ecosphere 7 (6), e01375. https://doi.org/ 10.1002/ecs2.1375.
- Gough, C.M., Bohrer, G., Hardiman, B.S., Nave, L.E., Vogel, C.S., Atkins, J.W., Bond-Lamberty, B., Fahey, R.T., Fotis, A.T., Grigri, M.S., Haber, L.T., Ju, Y., Kleinke, C.L., Mathes, K.C., Nadelhoffer, K.J., Stuart-Haëntjens, E., Curtis, P.S., 2021. Disturbance-accelerated succession increases the production of a temperate forest. Ecol. Appl. 31 (7), e02417 https://doi.org/10.1002/EAP.2417.
- Hardiman, B.S., Gough, C.M., Halperin, A., Hofmeister, K.L., Nave, L.E., Bohrer, G., Curtis, P.S., 2013. Maintaining high rates of carbon storage in old forests: A mechanism linking canopy structure to forest function. For. Ecol. Manage. 298, 111–119. https://doi.org/10.1016/j.foreco.2013.02.031.
- Harmon, M.E., Bond-Lamberty, B., Tang, J., Vargas, R., 2011. Heterotrophic respiration in disturbed forests: a review with examples from North America. J. Geophys. Res. Biogeosci. 116 (2) https://doi.org/10.1029/2010JG001495.
- Hendrickson, O.Q., Chatarpaul, L., Burgess, D., 2011. Nutrient cycling following wholetree and conventional harvest in northern mixed forest 19(6), 725–735. https://doi. org/10.1139/X89-112.
- Hillebrand, H., Langenheder, S., Lebret, K., Lindström, E., Östman, Ö., Striebel, M., O'Connor, M., 2018. Decomposing multiple dimensions of stability in global change experiments. Ecol. Lett. 21 (1), 21–30.
- Hocker Jr, H.W., Early, D.J., 1983. Biomass and leaf area equations for northern forest species. New Hampshire Agric. Experiment Station Univ. New Hampshire Res. Rep. 102, 27. https://doi.org/10.1093/forestry/cpt053.
- Janssens, I.A., Dieleman, W., Luyssaert, S., Subke, J.-A., Reichstein, M., Ceulemans, R., Ciais, P., Dolman, A.J., Grace, J., Matteucci, G., Papale, D., Piao, S.L., Schulze, E.-D., Tang, J., Law, B.E., 2010. Reduction of forest soil respiration in response to nitrogen deposition. Nature Geosci 3 (5), 315–322.
- Johnstone, J.F., Allen, C.D., Franklin, J.F., Frelich, L.E., Harvey, B.J., Higuera, P.E., Mack, M.C., Meentemeyer, R.K., Metz, M.R., Perry, G.L.W., Schoennagel, T., Turner, M.G., 2016. Changing disturbance regimes, ecological memory, and forest resilience. Front. Ecol. Environ. 14 (7), 369–378. https://doi.org/10.1002/FEE.1311.
- Ker, M.F., 1980. Tree biomass equations for seven species in southwestern New Brunswick. Tree Biomass Equations for Seven Species in Southwestern New Brunswick, No. M-X-114, 18.
- Kilburn, P.D., 1960. Effect of settlement on the vegetation of the University of Michigan Biological Station. Michigan Acad. Sci. Arts Lett. 45, 77–81.
- Lapin, M., Barnes, B.V., 1995. Using the Landscape Ecosystem Approach to Assess Species and Ecosystem Diversity. Conservat. Biol. 9 (5), 1148–1158. https://doi.org/ 10.1046/J.1523-1739.1995.9051134.X-I1.
- Lepistö, A., Futter, M.N., Kortelainen, P., 2014. Almost 50 years of monitoring shows that climate, not forestry, controls long-term organic carbon fluxes in a large boreal watershed. Glob. Change Biol. 20 (4), 1225–1237. https://doi.org/10.1111/ GCB.12491.
- Li, J., Pei, J., Liu, J., Wu, J., Li, B., Fang, C., Nie, M., 2021. Spatiotemporal variability of fire effects on soil carbon and nitrogen: A global meta-analysis. Glob. Change Biol. 27 (17), 4196–4206. https://doi.org/10.1111/GCB.15742.
- Liebman, E., Yang, J., Nave, L.E., Nadelhoffer, K.J., Gough, C.M., 2017. Research Article: Soil respiration in upper Great Lakes old-growth forest ecosystems. BIOS 88 (3), 105–115. https://doi.org/10.1893/0005-3155-88.3.105.
- Lindenmayer, D.B., Likens, G.E., Andersen, A., Bowman, D., Bull, C.M., Burns, E., Dickman, C.R., Hoffmann, A.A., Keith, D.A., Liddell, M.J., Lowe, A.J., Metcalfe, D.J., Phinn, S.R., Russell-Smith, J., Thurgate, N., Wardle, G.M., 2012. Value of long-term ecological studies. Austral Ecol. 37 (7), 745–757. https://doi.org/10.1111/J.1442-9993.2011.02351.X.

- Lorimer, C.G., Halpin, C.R., 2014. Classification and dynamics of developmental stages in late-successional temperate forests. For. Ecol. Manage. 334, 344–357. https://doi. org/10.1016/J.FORECO.2014.09.003.
- Luyssaert, S., Schulze, E.D., Börner, A., Knohl, A., Hessenmöller, D., Law, B.E., Ciais, P., Grace, J., 2008. Old-growth forests as global carbon sinks. Nature 455 (7210), 213–215. https://doi.org/10.1038/nature07276.
- Ma, W., Domke, G.M., Woodall, C.W., D'Amato, A.W., 2019. Land use changes, disturbances, and their interactions on future forest aboveground biomass dynamics in the Northern US. Forests 10 (7), 606. https://doi.org/10.3390/F10070606.
- Malamud, B.D., Millington, J.D.A., Perry, G.L.W., 2005. Characterizing wildfire regimes in the United States. Proc. Natl. Acad. Sci. 102 (13), 4694–4699. https://doi.org/ 10.1073/PNAS.0500880102.
- Marra, J.L., Edmonds, R.L., 1994. Coarse woody debris and forest floor respiration in an old-growth coniferous forest on the Olympic Peninsula, Washington, USA. Can. J. For. Res. 24 (9), 1811–1817. https://doi.org/10.1139/x94-234.
- Morin, R.S., Liebhold, A.M., Tobin, P.C., Gottschalk, K.W., Luzader, E., 2007. Spread of beech bark disease in the eastern United States and its relationship to regional forest composition. Can. J. For. Res. 37 (4), 726–736.
- Moritz, M.A., Parisien, M.-A., Batllori, E., Krawchuk, M.A., van Dorn, J., Ganz, D.J., Hayhoe, K., Moritz, M.A., Parisien, M.-A., Batllori, E., Krawchuk, M.A., van Dorn, J., Ganz, D.J., Hayhoe, K., 2012. Climate change and disruptions to global fire activity. Ecosphere 3 (6), 1–22. https://doi.org/10.1890/ES11-00345.1.
- Nave, L.E., Vance, E.D., Swanston, C.W., Curtis, P.S., 2009. Impacts of elevated N inputs on north temperate forest soil C storage, C/N, and net N-mineralization. Geoderma 153 (1–2), 231–240. https://doi.org/10.1016/j.geoderma.2009.08.012.
- Nave, L.E., Vance, E.D., Swanston, C.W., Curtis, P.S., 2010. Harvest impacts on soil carbon storage in temperate forests. For. Ecol. Manage. 259 (5), 857–866. https://doi.org/10.1016/J.FORECO.2009.12.009.
- Nave, L.E., Gough, C.M., Maurer, K.D., Bohrer, G., Hardiman, B.S., Le Moine, J., Munoz, A.B., Nadelhoffer, K.J., Sparks, J.P., Strahm, B.D., Vogel, C.S., Curtis, P.S., 2011. Disturbance and the resilience of coupled carbon and nitrogen cycling in a north temperate forest. J. Geophys. Res. Biogeosci. 116 (4), 4016. https://doi.org/ 10.1029/2011.IG001758.
- Nave, L.E., Gough, C.M., Perry, C.H., Hofmeister, K.L., le Moine, J.M., Domke, G.M., Swanston, C.W., Nadelhoffer, K.J., 2017. Physiographic factors underlie rates of biomass production during succession in Great Lakes forest landscapes. For. Ecol. Manage. 397, 157–173. https://doi.org/10.1016/J.FORECO.2017.04.040.
- Nave, L.E., le Moine, J.M., Gough, C.M., Nadelhoffer, K.J., 2019. Multidecadal trajectories of soil chemistry and nutrient availability following cutting vs. Burning disturbances in upper great lakes forests. Can. J. For. Res. 49 (7), 731–742. https://doi.org/10.1139/CJFR-2018-0211/SUPPL_FILE/CJFR-2018-0211SUPPLA.DOCX.
- Ontl, T.A., Janowiak, M.K., Swanston, C.W., Daley, J., Handler, S., Cornett, M., Hagenbuch, S., Handrick, C., McCarthy, L., Patch, N., 2020. Forest Management for Carbon Sequestration and Climate Adaptation. J. Forest. 118 (1), 86–101. https:// doi.org/10.1093/JOFORE/FVZ062.
- Pan, Y., Birdsey, R.A., Phillips, O.L., Jackson, R.B., 2013. The Structure, Distribution, and Biomass of the World's Forests. https://doi.org/10.1146/ANNUREV-ECOLSYS-110512-135914.
- Perala, D.A., Alban, D.H., 1993. Allometric biomass estimators for aspen-dominated ecosystems in the Upper Great Lakes. US Department of Agriculture Forest Service Research Paper, NC-134, 38. https://doi.org/10.2737/NC-RP-314.
- Pastorello, G., Trotta, C., Canfora, E., Chu, H., Christianson, D., Cheah, Y.-W. Poindexter, C., Chen, J., Elbashandy, A., Humphrey, M., Isaac, P., Polidori, D., Reichstein, M., Ribeca, A., van Ingen, C., Vuichard, N., Zhang, L., Amiro, B., Ammann, C., Arain, M.A., Ardö, J., Arkebauer, T., Arndt, S.K., Arriga, N., Aubinet, M., Aurela, M., Baldocchi, D., Barr, A., Beamesderfer, E., Marchesini, L.B., Bergeron, O., Beringer, J., Bernhofer, C., Berveiller, D., Billesbach, D., Black, T.A., Blanken, P.D., Bohrer, G., Boike, J., Bolstad, P.V., Bonal, D., Bonnefond, J.-M., Bowling, D.R., Bracho, R., Brodeur, J., Brümmer, C., Buchmann, N., Burban, B., Burns, S.P., Buysse, P., Cale, P., Cavagna, M., Cellier, P., Chen, S., Chini, I., Christensen, T.R., Cleverly, J., Collalti, A., Consalvo, C., Cook, B.D., Cook, D., Coursolle, C., Cremonese, E., Curtis, P.S., D'Andrea, E., da Rocha, H., Dai, X., Davis, K.J., Cinti, B.D., Grandcourt, A.d., Ligne, A.D., De Oliveira, R.C., Delpierre, N., Desai, A.R., Di Bella, C.M., Tommasi, P.d., Dolman, H., Domingo, F., Dong, G., Dore, S., Duce, P., Dufrêne, E., Dunn, A., Dušek, J., Eamus, D., Eichelmann, U., ElKhidir, H.A.M., Eugster, W., Ewenz, C.M., Ewers, B., Famulari, D., Fares, S., Feigenwinter, I., Feitz, A., Fensholt, R., Filippa, G., Fischer, M., Frank, J., Galvagno, M., Gharun, M., Gianelle, D., Gielen, B., Gioli, B., Gitelson, A., Goded, I., Goeckede, M., Goldstein, A.H., Gough, C.M., Goulden, M.L., Graf, A., Griebel, A., Gruening, C., Grünwald, T., Hammerle, A., Han, S., Han, X., Hansen, B.U., Hanson, C., Hatakka, J., He, Y., Hehn, M., Heinesch, B., Hinko-Najera, N., Hörtnagl, L., Hutley, L., Ibrom, A., Ikawa, H., Jackowicz-Korczynski, M., Janouš, D., Jans, W., Jassal, R., Jiang, S., Kato, T., Khomik, M., Klatt, J., Knohl, A., Knox, S., Kobayashi, H., Koerber, G., Kolle, O., Kosugi, Y., Kotani, A., Kowalski, A., Kruijt, B., Kurbatova, J., Kutsch, W.L., Kwon, H., Launiainen, S., Laurila, T., Law, B., Leuning, R., Li, Y., Liddell, M., Limousin, J.-M., Lion, M., Liska, A.J., Lohila, A. López-Ballesteros, A., López-Blanco, E., Loubet, B., Loustau, D., Lucas-Moffat, A., Lüers, J., Ma, S., Macfarlane, C., Magliulo, V., Maier, R., Mammarella, I., Manca, G., Marcolla, B., Margolis, H.A., Marras, S., Massman, W., Mastepanov, M., Matamala, R., Matthes, J.H., Mazzenga, F., McCaughey, H., McHugh, I., McMillan, A.M.S., Merbold, L., Meyer, W., Meyers, T., Miller, S.D., Minerbi, S., Moderow, U., Monson, R.K., Montagnani, L., Moore, C.E., Moors, E., Moreaux, V., Moureaux, C., Munger, J.W., Nakai, T., Neirynck, J., Nesic, Z., Nicolini, G., Noormets, A., Northwood, M., Nosetto, M., Nouvellon, Y., Novick, K., Oechel, W., Olesen, J.E., Ourcival, J.-M., Papuga, S.A., Parmentier, F.-J., Paul-Limoges, E., Pavelka, M., Peichl, M., Pendall, E., Phillips, R.P., Pilegaard, K., Pirk, N., Posse, G.,

- Powell, T., Prasse, H., Prober, S.M., Rambal, S., Rannik, Ü., Raz-Yaseef, N., Rebmann, C., Reed, D., Dios, V.R.d., Restrepo-Coupe, N., Reverter, B.R., Roland, M., Sabbatini, S., Sachs, T., Saleska, S.R., Sánchez-Cañete, E.P., Sanchez-Mejia, Z.M., Schmid, H.P., Schmidt, M., Schneider, K., Schrader, F., Schroder, I., Scott, R.L., Sedlák, P., Serrano-Ortíz, P., Shao, C., Shi, P., Shironya, I., Siebicke, L., Šigut, L., Silberstein, R., Sirca, C., Spano, D., Steinbrecher, R., Stevens, R.M., Sturtevant, C., Suyker, A., Tagesson, T., Takanashi, S., Tang, Y., Tapper, N., Thom, J., Tomassucci, M., Tuovinen, J.-P., Urbanski, S., Valentini, R., van der Molen, M., van Gorsel, E., van Huissteden, K.o., Varlagin, A., Verfaillie, J., Vesala, T., Vincke, C., Vitale, D., Vygodskaya, N., Walker, J.P., Walter-Shea, E., Wang, H., Weber, R., Westermann, S., Wille, C., Wofsy, S., Wohlfahrt, G., Wolf, S., Woodgate, W., Li, Y., Zampedri, R., Zhang, J., Zhou, G., Zona, D., Agarwal, D., Biraud, S., Torn, M., Papale, D., 2020. The FLUXNET2015 dataset and the ONEFlux processing pipeline for eddy covariance data. Sci. Data 7 (1).
- Peters, E.B., Wythers, K.R., Bradford, J.B., Reich, P.B., 2013. Influence of disturbance on temperate forest productivity. Ecosystems 16 (1), 95–110. https://doi.org/10.1007/s10021-012-9599-y.
- Scheuermann, C.M., Nave, L.E., Fahey, R.T., Nadelhoffer, K.J., Gough, C.M., 2018.
 Effects of canopy structure and species diversity on primary production in upper Great Lakes forests. Oecologia 188 (2), 405–415. https://doi.org/10.1007/s00442-018.4265.r.
- Schmid, A.V., Vogel, C.S., Liebman, E., Curtis, P.S., Gough, C.M., 2016. Coarse woody debris and the carbon balance of a moderately disturbed forest. For. Ecol. Manage. 361, 38–45.
- Schmitt, M.D.C., Grigal, D.F., 1981. Generalized biomass estimation equations for Betula papyrifera Marsh. Can. J. For. Res. 11 (4), 837–840. https://doi.org/10.1139/x81-122
- Seidl, R., Spies, T.A., Peterson, D.L., Stephens, S.L., Hicke, J.A., Angeler, D., 2016.
 REVIEW: Searching for resilience: addressing the impacts of changing disturbance regimes on forest ecosystem services. J. Appl. Ecol. 53 (1), 120–129.
- Seneviratne, S.I., Nicholls, N., Easterling, D., Goodess, C.M., Kanae, S., Kossin, J., Luo, Y., Marengo, J., McInnes, K., Rahimi, M., Reichstein, M., Sorteberg, A., Vera, C., Zhang, X., 2012. Changes in climate extremes and their impacts on the natural physical environment. In: Managing the Risks of Extreme Events and Disasters to Advance Climate Change Adaptation [Field, C.B., Barros, V., Stocker, T.F., Qin, D., Dokken, D. J., Ebi, K.L., Mastrandrea, M.D., Mach, K.J., Plattner, G.-K., Allen, S.K., Tignor, M., Midgley, P.M. (Eds.)]. A Special Report of Working Groups I and II of the Intergovernmental Panel on Climate Change (IPCC). Cambridge University Press, Cambridge, UK, and New York, NY, USA, pp. 109-230. https://doi.org/10.7916/d8-6nbt-s431.
- Shiklomanov, A.N., Bond-Lamberty, B., Atkins, J.W., Gough, C.M., 2020. Structure and parameter uncertainty in centennial projections of forest community structure and carbon cycling. Glob. Change Biol. 26 (11), 6080–6096. https://doi.org/10.1111/ GCB 15164
- Smith, E.A., O'Loughlin, D., Buck, J.R., St. Clair, S.B., 2011. The influences of conifer succession, physiographic conditions and herbivory on quaking aspen regeneration after fire. Forest Ecol. Manage. 262 (3), 325–330. https://doi.org/10.1016/J. FORECO 2011 03 038
- Stuart-Haëntjens, E.J., Curtis, P.S., Fahey, R.T., Vogel, C.S., Gough, C.M., 2015. Net primary production of a temperate deciduous forest exhibits a threshold response to increasing disturbance severity. Ecology 96 (9), 2478–2487. https://doi.org/ 10.1890/14-1810.1.
- Tang, J., Bolstad, P.V., Martin, J.G., 2009. Soil carbon fluxes and stocks in a Great Lakes forest chronosequence. Global Change Biol. 15 (1), 145–155. https://doi.org/ 10.1111/J.1365-2486.2008.01741.X.
- Tang, J., Bolstad, P.V., Desai, A.R., Martin, J.G., Cook, B.D., Davis, K.J., Carey, E.V., 2008. Ecosystem respiration and its components in an old-growth forest in the Great Lakes region of the United States. Agric. For. Meteorol. 148 (2), 171–185.
- Ter-Mikaelian, M.T., Korzukhin, M.D., 1997. Biomass equations for sixty-five North American tree species. For. Ecol. Manage. 97 (1), 1–24. https://doi.org/10.1016/S0378-1127(97)00019-4.
- Thom, D., Seidl, R., 2016. Natural disturbance impacts on ecosystem services and biodiversity in temperate and boreal forests. Biol. Rev. 91 (3), 760–781. https://doi. org/10.1111/BRV.12193.
- Ueyama, M., Iwata, H., Nagano, H., Tahara, N., Iwama, C., Harazono, Y., 2019. Carbon dioxide balance in early-successional forests after forest fires in interior Alaska. Agric. For. Meteorol. 275, 196–207. https://doi.org/10.1016/J. AGRFORMET.2019.05.020.
- Wales, S.B., Kreider, M.R., Atkins, J., Hulshof, C.M., Fahey, R.T., Nave, L.E., Nadelhoffer, K.J., Gough, C.M., 2020. Stand age, disturbance history and the temporal stability of forest production. For. Ecol. Manage. 460, 117865.
- Walker, L.R., Wardle, D.A., Bardgett, R.D., Clarkson, B.D., 2010. The use of chronosequences in studies of ecological succession and soil development. J. Ecol. 98 (4), 725–736. https://doi.org/10.1111/j.1365-2745.2010.01664.x.
- White, L.L., Zak, D.R., Barnes, B.V., 2004. Biomass accumulation and soil nitrogen availability in an 87-year-old Populus grandidentata chronosequence. For. Ecol. Manage. 191 (1–3), 121–127. https://doi.org/10.1016/j.foreco.2003.11.01.
- Whitney, G.G., 1987. An ecological history of the great lakes forest of Michigan. J. Ecol. 75 (3), 667. https://doi.org/10.2307/2260198.

Wiant, H.V., 1977. Tables and procedures for estimating weights of some Appalachian hardwoods. West Virginia Agric. For. Experiment Station Bull. 659, 36. https://doi.org/10.33915/agnic.65.

Williams, C.A., Gu, H., Jiao, T., 2021. Climate impacts of U.S. forest loss span net warming to net cooling. *Science*. Advances 7 (7), 8859–8871. https://doi.org/ 10.1126/SCIADV.AAX8859/SUPPL_FILE/AAX8859_SM.PDF. Young, H.E., Ribe, J.H., Wainwright, K., 1980. Weight tables for tree and shrub species in maine. Life Sci. Agric. Experimental Station, Univ. Maine Orono Miscellaneous Rep. 230, 84 pp.